Tutorial on LTE/LTE-A Cellular Network Dimensioning using Iterative Statistical Analysis

Mona Jaber[1], **Zaher Dawy**[1], **Naeem Akl**[1], **and Elias Yaacoub**[2,3]

[1] Electrical and Computer Engineering Department, American University of Beirut, Beirut, Lebanon.

Email: {mtj00, zd03, nka16}@aub.edu.lb

[2] Strategic Decisions Group (SDG), Beirut, Lebanon.

[3] Faculty of Computer Studies, Arab Open University (AOU), Tayouneh, Beirut, Lebanon.

Email: eliasy@ieee.org

Abstract

LTE is the fastest growing cellular technology and is expected to increase its footprint in the coming years, as well as progress towards LTE-A. The race among operators to deliver the expected quality of experience to their users is tight, and demands sophisticated skills in network planning. Radio network dimensioning (RND) is an essential step in the process of network planning, and has been used as a fast, but indicative, approximation of radio site count. RND is a pre-requisite to the lengthy process of thorough planning. Moreover, results from RND are used by players in the industry, to estimate pre-planning costs of deploying and running a network; thus, RND is, as well, a key tool in cellular business modelling. In this work, we present a tutorial on radio network dimensioning, focused on LTE/LTE-A, using an iterative approach to find a balanced design that mediates among the three design requirements: coverage, capacity, and quality. This approach uses a statistical link budget analysis methodology, which jointly accounts for small and large scale fading in the channel, as well as loading due to traffic demand, in the interference calculation. A complete RND manual is thus presented, which is of key importance to operators deploying or upgrading LTE/LTE-A networks for two reasons. It is purely analytical, hence it enables fast results, a prime factor in the race undertaken. Moreover, it captures essential variables affecting network dimensions, and manages conflicting targets to ensure user quality of experience; another major criterion in the competition. The described approach is compared to the traditional RND, using a commercial LTE network planning tool. The outcome further dismisses the traditional RND for LTE, due to unjustified increase in number of radio sites and related cost, and motivates further research in developing more effective and novel RND procedures.

Index Terms

Link budget analysis, iterative radio network dimensioning, cellular network planning, inter-cell interference statistics, LTE/LTE-A

I. Introduction

Cellular radio network planning in general, is the process of selecting the minimum radio site positions, and corresponding parameters and optional features to provide adequate service to all subscribers. Cellular technology is evolving, and new cellular

generations often require smaller cells. Nevertheless, incumbent operators prefer to reuse existing radio sites and fill the gap with new sites. In this context, radio network planning concerns maximising the number of reused radio sites and identifying the minimum number and location of new radio sites [1]. In general, the three planning objectives: coverage, capacity and quality of service (QoS) are often inter-dependent and interrelated; hence, they need to be addressed jointly. A radio network planning exercise is limited to a given area (e.g., town, city, country, etc.); coverage targets refer to the percentage of the area covered, or the percentage of population in the area covered. A point in the area is considered covered, if a user in this location is able to establish a reliable voice or data session at the desired rate on both uplink and downlink directions. For instance, in 2013, London had 97.9% area coverage and 99.7% population coverage; whereas Edinburgh had 77.3% and 98.2%, respectively [2]. Capacity targets may be defined as the number of active calls, data sessions, or total throughput per cell, depending on the cellular technology. Quality targets reflect the users' satisfaction, hence depend on the cellular technology considered. Blocking probability is used for fixed rate circuit switched access systems; user data rate is used for packet switched systems.

A dominant objective in RND is to minimise the cost of the network design, however there is an inherent trade-off, common to all communication systems, that also exists between capacity, coverage and quality. In other words, for a given fixed cost, the RND may be designed in a multitude of ways, whereby each design reflects a different level of trade-off between coverage, capacity and quality. For example, for that cost, a cellular operator may decide to have sporadic coverage of selected hot-spots with limited coverage, controlled capacity, and high quality. Alternatively, for the same cost, another cellular operator may choose to maximise its footprint at the expense of quality and/or capacity. But the problem can also be addressed from a different perspective; assuming that the percentage of area (or population) covered is imposed by the spectrum licensing agreement, for instance, the RND may be designed in various ways based on different trade-off equilibriums. A minimum number of high power macro-cells with large spectrum allocation may be deployed, thus limiting the deployment cost but potentially compromising quality of service due to high inter-cell interference. Another option would be to increase number of macro-cells operating at less power, hence limiting the inter-cell interference, at the cost of higher expenditures. In this work we address these various trade-off and demonstrate their importance by comparing the cost-related metrics of different designs; hence the trade-off between quality and cost is also emphasized and central to the paper.

RND is the first step in radio planning, and is traditionally centred around the link budget analysis (LBA), a radio site count estimating tool. The raw outcome of the LBA is the maximum allowed path loss. This is used with a propagation model, to estimate the maximum cell coverage range, which is then used to estimate the minimum required radio site density. A cell, traditionally, represents an area covered by one antenna such as a sector in a sectored radio site. A radio site is the location of the radio access equipment and antennas; in LTE it is the evolved Node B or eNB. LBA is enabled by some simplified assumptions concerning heights, clutter types, and traffic distribution, as shown in Figure 2. The statistical propagation model used in LBA, does not include terrain height effects, but, often has a slope and intercept value for each type of environment, otherwise referred to as clutter type (e.g., urban, sub-urban, rural). Furthermore, the planning area is divided into few homogeneous and continuous subareas, that are

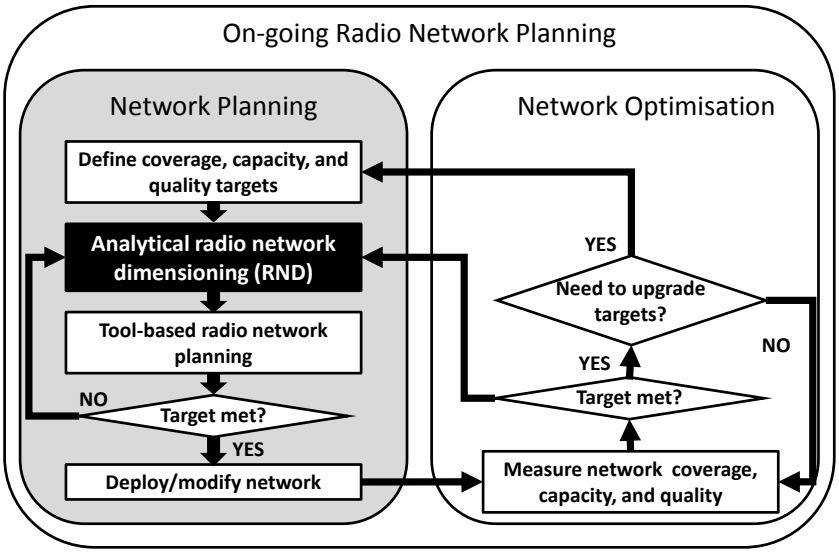

Fig. 1. Radio network planning is an ongoing task that iterates between planning and optimisation. The RND process is an essential step in radio planning; it is also the initial site count estimation tool.

depicted by one clutter type. Also, in the LBA phase, users are assumed identical and uniformly distributed within each subarea in the network; thus, leading to uniform traffic distributions and equally loaded base stations. This fairly simplified approach allows, nevertheless, for a quick analysis and an indication of eNB count. The authors in [3] use conformal mapping to transform the actual traffic distribution through canonical domains to a symmetrical scenario; then, they use a common RND approach to identify the number and canonical location of base stations, followed by an inverse transformation function to find the corresponding realistic locations. The LBA also provides valuable insight into the effects of different parameters and features on network performance.

The LBA process is described in [4], [5], and [6] in the context of second cellular generation 2G/GSM (global system for mobile communication), 3G/UMTS (universal mobile telecommunications system), and 4G/LTE-A (long term evolution advanced), respectively. However, authors in [6], readopt 3G assumptions without derivations or validations; consequently, their traditional approach is unable to accurately capture the tradeoffs between coverage, capacity and quality in LTE/LTE-A. RND results have direct implications on operational and capital expenditure of an operator, ergo it is crucial to reflect the impact of various design targets (coverage/capacity/quality centric) in the business plan.

The second step in radio network planning is the tool-based planning, traditionally performed using commercial planning tools to perform detailed predictions (see Figure 1). In these tools, the propagation model takes into account the characteristics of the selected antenna, the terrain elevation, and the land use and land clutter surrounding each eNB. Moreover, an elaborate traffic modelling application is employed to represent, realistically, users' positions in the network and their different traffic profiles as shown in Figure 2. The tool-based planning exercise takes the output of the RND as a starting point; at the end of the process the number of radio sites and locations would be optimised further, based on more realistic assumptions. Monte Carlo simulations are performed to derive network performance indicators. Accordingly, the setting of parameters, such as radio site location, antenna azimuth and tilt, neighbouring and mobility parameter settings, and frequency planning (if applicable), can be adjusted in order to reach desired targets. Results obtained from an effective and successful RND exercise present a good starting point to the

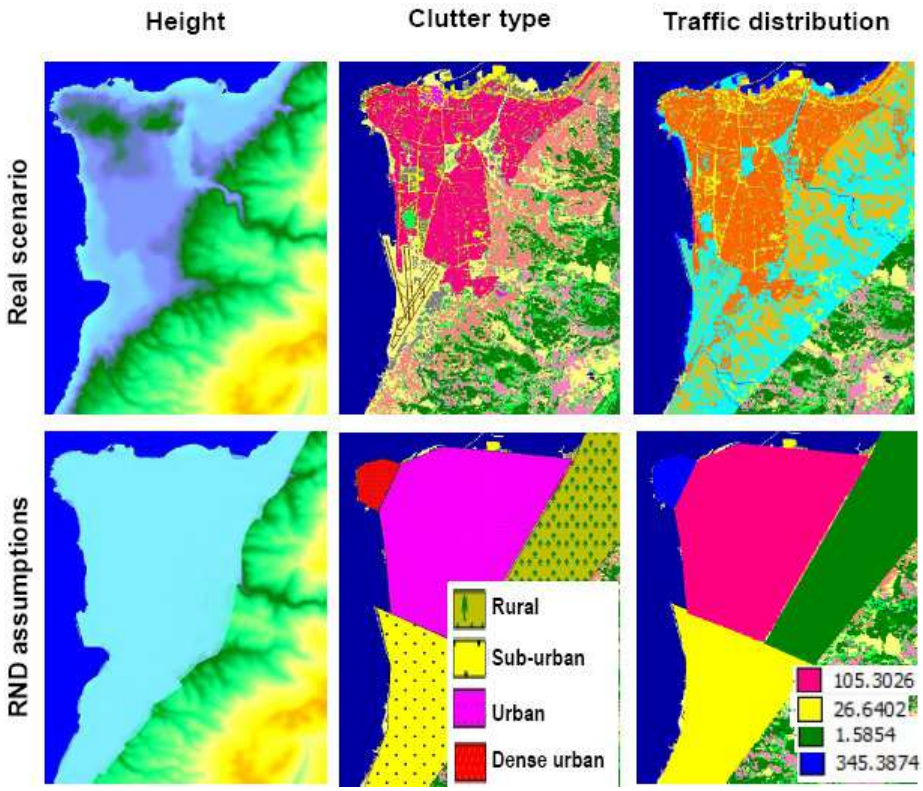

Fig. 2. Major assumptions facilitate the LBA-based RND process. Firstly, heights are ignored, thus the area is considered flat. Second, the target area is divided into subareas, each belonging to a clutter class with specific propagation models. Lastly, traffic maps are uniform within each subarea ($\mathrm{kbps/km^2}$).

tool-based planning phase, and often require minimal adjustments to meet the design targets in the realistic settings. Thus, the tool-based planning step is a practical validation test to the correctness and preciseness of the RND approach.

Radio network planning is an on-going activity in a live network. The post-deployment planning objective is to optimise the network in view of the changing environment such as: increase in users, improved data rate, and new services. Ideally, the RND and planning tool are updated with live network data and used to identify a proper optimisation technique prior to implementation (see Figure 1). Such an approach avoids unnecessary outages and network performance degradation, and ensures users quality of service through the optimisation phase. Thus, RND and tool-based planning do not end upon network deployment, but are continuously revisited during the network's lifetime.

In this paper, we present a tutorial on the LTE network RND process through an original analytical approach that highlights LTE tradeoffs. An LBA built on analytical methodologies with no requirement for simulations presents a key advantage because of its ability to yield fast results that are essential for network planning and business modelling. Accordingly, it has been the norm, in previous cellular generations' LBAs, to represent the effect of random variables, such as fading, through statistical power margins which are typically derived from simulation results compiled into lookup tables [7]. Effectively, this approach is not valid for LTE since the intrinsic flexible nature of LTE and its advanced features result in a multitude of lookup tables, hence rendering this circumvention quite impractical. In this tutorial, we demonstrate that a short-cut pragmatic setting of such parameters may lead to wrong results, and emphasise the importance of developing a statistical RND process in the context of LTE, inviting more research in this domain. It should be noted that throughout this paper, the term fading is used to refer to joint small and large scale fading

which are often termed fast fading (Rayleigh/Rician) and slow fading (shadowing), respectively.

A. Literature review

A thorough investigation into published material indicates that this work is the first to offer a comprehensive tutorial on analytical RND with focus on LTE/LTE-A. Authors in [6] dedicate a whole chapter to LTE RND, however, the process of dimensioning, as part of the bigger network planning procedure, and the derivations and implications of pertinent entities affecting the network dimensions are not comprehensively covered. Upase et al. in [8] provide a brief description of the network dimensioning and planning procedure for WiMAX from an implementation perspective, however, it lacks supporting information of theoretical background and link budget derivations.

Some recent papers tackle LTE-specific RND from different perspectives. An analytical model for orthogonal frequency- division multiple access (OFDMA) dimensioning is proposed in [9] to find the minimum number of channels required to guarantee a minimum loss probability. The model considers an isolated cell to estimate the number of required sub-channels per user depending on the signal to noise ratio (SNR), in which the signal is affected by large scale fading. Simulations, instead of analytical modelling, are often used for dimensioning such as [10] and [11]. Authors in [10] propose an in-house simulation tool for LTE coverage and capacity dimensioning, and a resulting analysis on the effect of height and clutter types on cell range. The simulations are, however, based on path loss averages, thus large and small scale fading are ignored. A recent work, [11], looks at using capacity dimensioning results in order to find suitable solutions for network evolution. The authors extend usage of known propagation models to a refined statistical method to evaluate two possible network densification approaches: adding macro-cells or small cells, depending on the city model and traffic distribution. Another work, related to re-dimensioning for improving QoS, is presented in [12]. The authors investigate how QoS affects network capacity dimensions and at which stage the network should be extended. However, the model focuses on control overheads, and ignores channel fading and other cell interference in the dimensioning calculations.

Research on the LBA part of the RND has, perhaps, received more attention than the full RND topic. There are a few research papers that propose an LTE perspectives to the traditional analytical LBA; we identify them as the traditional research direction. Two other directions look at the outage analysis of OFDMA technologies, one based on a single sub-carrier scenario and another on a multi sub-carrier scenario.

The traditional research direction readopted the traditional dimensioning approach of 2G and 3G networks on LTE such as [6], [13]–[15]; therefore adjusting the LBA with LTE specific fading and interference statistical margins. However, LTE's claim to increased spectral efficiency is based on the network's capability to adapt fast to signal-to-interference-plus-noise ratio (SINR) fluctuations. Moreover, LTE's flexibility in adaptive modulation and coding as well as multiple antenna techniques results in a myriad of possibilities hence an unmanageable number of entries in the lookup tables. Subsequently, the previously accepted detour is no longer practical for LTE; therefore, there is a need to accurately and statistically capture the effect of variables such as fading and loading in the LBA.

Another research direction models the system interference considering a single sub-carrier scenario. For example, Seol et al.

in [16] and [17] propose an elaborate derivation of inter-cell interference (ICI) probability density function under multi-path Rayleigh and Ricean small scale fading respectively, conditioned on the large scale fading and the network load. Their objective is to point out the inaccuracy of assuming Gaussian ICI and its effect on transmitter and receiver design in OFDMA. The approach is thus complex and relies on Monte Carlo simulations to derive averages, hence not suitable for dimensioning purposes. On the other hand, Ben Cheick et al. in [18] propose an outage probability analysis based on the statistical modelling of the downlink interference using two approaches: the Fenton-Wilkinson and the central limit theorem. They reach mathematically manageable equations but in the process, approximate small scale fading effect of interfering cells' channels to their average value, and consider full cell load. Tabassum et al. in [19] capture accurately the effect of composite fading (i.e., small and large scale fading) on the channels from the serving cell and interfering cells, while accounting for the scheduling algorithm impact on ICI. The analysis provides estimations of the outage probability and the cell ergodic capacity but does not proceed to use the outcome for dimensioning purposes. Yang and Fapojuwo in [20] propose an analytical framework for a hexagonal cellular network with Rayleigh small scale fading, and consequently, derive corresponding coverage probability and the spectrum efficiency characterisation. Another milestone research in this field is by Andrews et al. in [21], in which general models for multi-cell SINR are presented using stochastic geometry, and assuming base stations' locations follow a Poisson distribution as opposed to fixed grid. Tractable models are proposed with simplifying assumptions such as Rayleigh channels and negligible thermal noise; results from these are compared to numerical models with more realistic assumptions. The work is valuable in defining a new line of research, however, the models proposed are not applicable to the LTE RND exercise in their presented form. Although final planning designs are often non-grid as a result of site acquisition constraints, it cannot be considered as a given in the RND phase. This additional layer of complexity is often part of planning and is considered to be an outcome of the planning process, not an input to it. Single sub-carrier ICI estimation is an essential milestone in the RND exercise but is also a critical part in the evaluation of innovative features for interference mitigation such as inter-cell interference coordination, e.g., [22].

A third research direction is based on a statistical interference model with multiple sub-carrier considerations. Guiliano and Mazenga in [23] base their approach on the exponential effective SINR model, as in [24] and [25], approximated by a Gaussian random variable. The approach however is complex and still relies on simulations while ignoring large scale fading. Kelif et al. in [26] propose an approach based on the mean instantaneous capacity concept as in [25] using the Fenton-Wilkinson method to approximate the joint effect of large and small scale fading on the SINR distribution but with similar assumptions, as in [18], thus, assuming full cell load.

B. Contributions

The main contribution of this work is that it presents the first comprehensive LTE/LTE-A radio network dimensioning tutorial. To the best of our knowledge, it is the first tutorial to tackle the practical derivations and implications of LTE RND, based on thorough statistical modelling of pertinent radio aspects. We use an original approach to highlight the paradigm of LTE RND, through performance analysis and a case study, to motivate new research in this direction. To this end, another contribution of the

paper is the presented statistical based dimensioning approach accompanied by results, analysis, and insights for various parameters and scenarios. Inasmuch, this tutorial has two main aims:

1) The first objective it to provide engineers in industry with a compact overview of the process of radio network dimensioning that is used by cellular operators globally to dimension hundreds of networks that serve billions of subscribers. This overview is supported by mathematical analysis and performance results that can provide useful practical insights and highlight limitations of existing methodologies. Indeed, a reliable RND approach is a key engine for operators competing for quality of service delivery, and for tool developers offering cutting edge features, as well as for telecommunication vendors and consultants dimensioning their business plan.
2) The second objective is to trigger more research in this area by highlighting the limitations of the traditional approach and providing a road-map for a new approach based on statistical interference modelling, while effectively capturing fading dynamics on serving and interfering cells as well as the effect of cell loading on levels of interference from neighbouring cells. The presented approach improves on traditional methods by deriving LTE-specific LBA parameters (e.g., linking the interference degradation margin to the actual cell loading on neighbouring cells and corresponding channel fading). A case study is presented with derivations, results, analysis, and insights, to demonstrate the benefits of the statistical approach. Such results aim at promoting the usage of statistical analysis in RND, especially when addressing advanced features as detailed in Section VII.

In this paper, we first present a methodology description of the statistical LBA process, backed with derivations and interpretations of key factors affecting LTE/LTE-A design. Then, a practical implementation of the methodology is provided, leading to a detailed analysis of LTE/LTE-A design tradeoffs. In this exercise, crucial characteristics of the technology are framed such as cell breathing and elasticity, effect of inter-site distance on edge user experience, and relation between transmit power and cell range. Subsequently, the tutorial describes the integration of the statistical LBA in the iterative RND process, to balance the conflicting dimensioning requirements of coverage, capacity and quality. A case study is then presented, with the objective of comparing the presented RND to the traditional RND, by conducting tool-based simulations for each, using a commercially planning tool. This section details the method of data migration to the planning tool, in addition to guidelines for interpreting simulation results and comparing the simulated network performance to the design targets. The case study shows that the traditional RND results in 36% unnecessary extra eNBs, and a network performance that exceeds the targets; whereas the statistical-LBA-based approach yields performance indicators close to the initial targets. Additional eNBs require higher capital expenditure (CapEX) due to the cost of building and installation, and an increase in operational expenditure (OpEX) due to the additional maintenance and operational bills. Such an increase in cost motivates more research in the domain of LTE RND, to provide various parties in the industry with a reliable procedure for technical and business dimensioning.

The rest of the paper is organized as follows. Section II gives a background on link budget analysis highlighting the traditional approach and LTE specific parameters. Section III presents the derivations leading to the statistical link budget analysis (SLBA).

Corresponding results and insights learned from the presented approach are discussed in Section IV. Section V presents an iterative dimensioning process for LTE based on SLBA. A case study comparing the traditional RND to the approach presented, using a commercial planning tool, is presented in Section VI. Finally, Section VII summarizes the tutorial and highlights key challenges in future dimensioning of future networks.

C. Mathematical notations

Mathematical notations and parameters are listed in Table I for clarity. As a convention, variables that are interchangeably used in linear form (X) and in logarithmic form are presented with ($\breve{X}$) when expressed in dB or dBm, e.g., L_s is the path loss between the user and the severing eNB in linear form (i.e. ratio) and $\breve{L}_s$ is the same entity expressed in dB, whereas P' is the total transmit power in Watts and $\breve{P}'$ is the same power in dBm. Another notation convention adopted in this work is that the subscript x in X_x indicates the concerned eNB, e.g., A_s refers to the fading variable on the downlink channel from the serving eNB, whereas L_n refers to the path loss from the neighbouring eNB n.

II. Radio Network Dimensioning (RND)

RND forms the initial stage in network planning and, traditionally, it has consisted of two main processes: coverage planning using the LBA, and capacity planning using Erlang equations for GSM [27] or Shannon and pole capacity equations for spread spectrum technologies [28]. Often the two processes are iteratively revisited, especially with spread spectrum radio access, to find an RND solution that balances coverage and capacity. LBA is centred on Reudink's identified deterministic relationship between cell edge coverage probability/reliability (ECP) and area coverage probability/reliability (ACP) [29]. Cell edge reliability refers to the probability that the radio frequency signal strength measured on the contour at the cell edge will meet, or exceed, a desired quality threshold (e.g., -90dBm). Whereas, cell area reliability is the probability that the signal will meet, or exceed, the quality threshold after integrating the contour probability over the entire area of the cell. Because of this relationship, estimating the distance to the cell edge can be shown to be theoretically equivalent to determining the reliability of the signal strength within the cell [29].

A. Traditional link budget analysis

The link budget analysis is a traditional tool used to compute the maximum allowed path loss (MAPL) between the base station transmitter (TX) and the mobile receiver (RX) at the cell edge, as shown in Figure 3. The MAPL is then translated into a cell range using the propagation equation, looking at both the uplink (UL) and the downlink (DL) directions. A typical LTE DL budget is presented in Table II, where parameters have been grouped into those that are considered constants, and those that are considered random variables. Referring to Table II, and starting with the maximum power at the base station, the effective isotropic radiated power (EiRP) is first calculated accounting for all gains and losses in the transmitter antenna chain. The EiRP per sub-carrier ($\breve{P}$) is then obtained by assuming that power is distributed equally over the number of available sub-carriers. Then, thermal noise power in a sub-carrier ($\breve{\sigma}^2$) is computed given the thermal noise power spectral density and sub-carrier bandwidth. The basic SNR is

TABLE I
TABLE OF MATHEMATICAL SYMBOLS.

Parameters	Description
A	Fading gain component
α	Path loss exponent
B_1	Cable/connector/combiner losses
B_2	Receive noise figure
B_3	Penetration loss
D_S	Subscriber density
D_{sub}	Number of sub-carriers
Δ_R	Accepted difference between r_A and r_S in iterative approach
Δ_η	Accepted difference between η_A and η_C in iterative approach
E	Total effective isotropic radiated power (EiRP)
$f_X(x)$	Probability distribution function of variable X
γ	Signal-to-interference-plus-noise ratio (SINR)
γ'	Signal-to-noise ratio (SNR)
$g()$	Gamma function
G_R	Receive antenna gain
G_T	Transmit antenna gain
η	Cell load
η_A	Assumed cell load in iterative approach
η_C	Capacity cell load in iterative approach
I	Total interference
I_n	Interference from neighbouring cell n
K	Path loss constant
λ_n	Expected value of I_n
L	Mean path loss
$L_{\max}$	Maximum allowed path loss (MAPL) of a cell having inter-cell interference
$L'_{\max}$	MAPL in case of isolated cell
μ	Interference degradation component
$M_{B_{\mathrm{total}}}$	Total losses
M_f	Fading margin
$M_{G_{\mathrm{total}}}$	Total gains
M_μ	Interference degradation margin
N	Number of cells in the network
P'	Total transmit power in Watts
P	EiRP per sub-carrier
R	Cell range in km
r_A	Assumed cell range in iterative approach
r_S	Safe cell range that leads to the required edge coverage probability in iterative approach
S	Received signal strength
σ^2	Total thermal noise power in channel
T	Effective transmit power per sub-carrier
θ	Thermal noise power spectral density
U	Number of subscribers per eNB
W	Bandwidth per sub-carrier in Hz

computed by taking the ratio of received signal strength to the thermal noise power in the channel. However, a realistic amplifier (the mobile receiver in the DL budget) also adds some extra noise from its own components and degrades the SNR ratio; thus the SNR at the output of the amplifier is worse than the SNR at its input. In other words, if the target SNR ($\breve{\gamma}'_{\mathrm{target}}$) is -9.1dB and the noise figure of the mobile device is 7dB, then the SNR at the input of the mobile receiver should be -2.1dB. In addition, often other constraints are included in the LBA to account for signal absorption loss in designs that are targeted for indoor or in-car receivers, referred to as penetration loss in Table II.

Two essential design margins remain unaccounted for: the fading margin ($\breve{M}_f$) and the interference degradation margin ($\breve{M}_\mu$). These design margins are shown in the variable parameters section of the link budget and are given special attention in designing

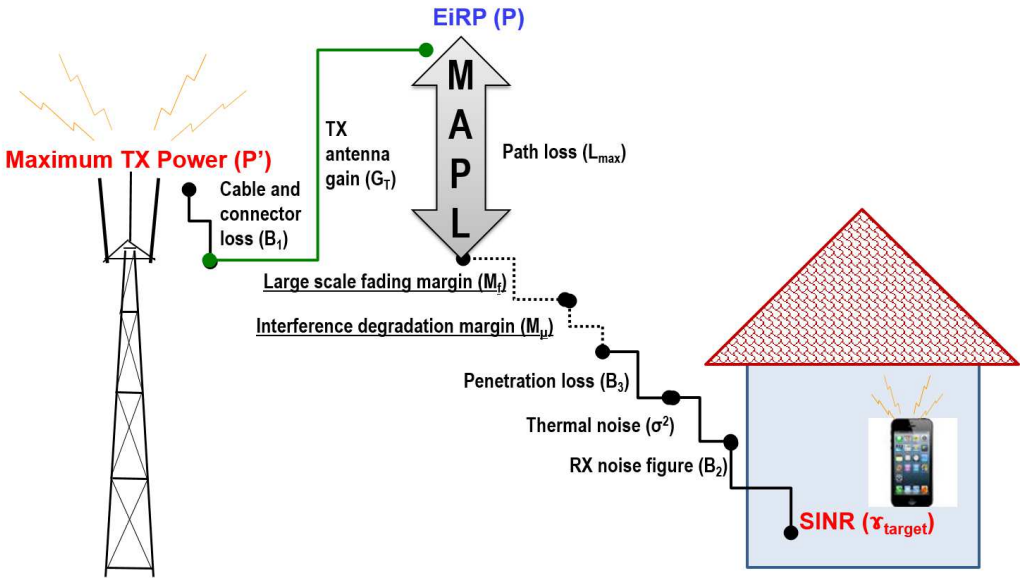

Fig. 3. This figure represents the losses and gains encountered by the signal from the transmitter to the receiver. In order to find the maximum allowed path loss, we assume maximum transmit power and minimum required SINR at the receiver. The gains and losses that can be assumed deterministic are presented in solid lines; whereas the statistical variables, such as large scale fading and interference degradation margins, are shown in dotted lines.

the LTE link budget, as will be discussed in coming sections. The fading margin is a deterministic power margin that compensates for signal variation due to statistical fading distribution and, thus, used to improve cell edge reliability. The interference degradation margin, is the degradation of the SNR in the presence of in-band interfering neighbouring cells causing ICI. It should be noted that in some literature, the term noise rise is used instead of interference degradation. For instance, consider an interference degradation margin equal to 3dB in the downlink budget. This indicates that, an isolated base station that can provide an SNR of -2.1dB to users at its cell edge, would only offer an SINR of -5.1dB in the presence of interfering neighbours. In LTE, the interference from other cells is due to the fact that all cells are continuously sharing the spectrum, thus, the level of interference is tied to the level of activity in neighbouring interfering cells (higher activity results in higher probability of using the same sub-carriers).

B. Propagation model characteristics

The mean path loss between the base station and a receiver at the cell edge is expressed as in (1). Consequently the received power at the cell edge can be expressed as shown below, where $\breve{S}$ is the received power in dBm, $\breve{T}$ is the effective transmit power of the base station, $\breve{L}$ is the mean path loss in dB, R is the cell range in km, $\breve{K}$ and α are the path loss constant and path loss exponent, respectively [30]. In (2), the variable $\breve{A}$ captures the signal variations due to fading; thus, the received signal is not deterministic but follows a statistical distribution governed by the channel fading characteristics.

$$\breve{L} = \breve{K} - 10\alpha \cdot \log_{10}(R) \tag{1}$$

$$\breve{S} = \breve{T} - \breve{L} + \breve{A} = \breve{T} - (\breve{K} - 10\alpha \cdot \log_{10}(R)) + \breve{A} \tag{2}$$

Figure 4 (right) represents an instantaneous snapshot of an omnidirectional cell edge where the random dotted line represents the points that satisfy the target signal strength (e.g., -90dBm). Figure 4 (left) depicts the statistical distribution of the signal strength at the cell edge around a normalised mean. In this figure, the channel fading characteristics are restricted to large scale fading which is

TABLE II
TYPICAL LTE DOWNLINK LINK BUDGET ANALYSIS (LBA).

Constant parameters	**Unit**	**Formula**	**Value**
Total transmit power	dBm	$\breve{P}'$	46
Transmit antenna gain	dBi	$\breve{G}_T$	18
Cable/connector/combiner losses	dB	$\breve{B}_1$	2.5
EiRP	dBm	$\breve{E} = \breve{P}' + \breve{G}_T - \breve{B}_1$	61.5
Total number of sub-carriers	10MHz	D_{sub}	600
EiRP per sub-carrier	dBm	$\breve{P} = 10 \cdot \log(\frac{E}{D_{\text{sub}}})$	33.7
Thermal noise density	dBm/Hz	$\breve{\theta}$	-173.8
Bandwidth per sub-carrier	Hz	W	15000
Total thermal noise in channel	dBm	$\breve{\sigma}^2 = \breve{\theta} + 10 \cdot \log(W)$	-132.0
Receive antenna gain	dBi	$\breve{G}_R$	0
Receive noise figure	dB	$\breve{B}_2$	7
Required SNR target	dB	$\breve{\gamma}'_{\text{target}}$	-2.1
Penetration loss	dB	$\breve{B}_3$	18
Total gains	dB	$\breve{M}_{G_{\text{total}}} = \breve{G}_R$	0
Total losses	dB	$\breve{M}_{B_{\text{total}}} = \breve{B}_2 + \breve{B}_3$	25
Effective power per sub-carrier	dB	$\breve{T} = \breve{P} + \breve{M}_{G_{\text{total}}} - \breve{M}_{B_{\text{total}}}$	8.7
Variable parameters	**Unit**	**Formula**	**Value**
Fading margin	dB	$\breve{M}_f$	5
Interference degradation margin	dB	$\breve{M}_\mu$	2
Dimensioning results	**Unit**	**Formula**	**Value**
MAPL	dB	$\breve{L}_{\max} = \breve{T} - (\breve{\gamma}'_{\text{target}} + \breve{\sigma}^2 + \breve{M}_f + \breve{M}_\mu)$	135.8
Cell range	km	$R = 10^{\frac{\breve{L}_{\max} - \breve{K}}{-10 \cdot \alpha}}$	0.931

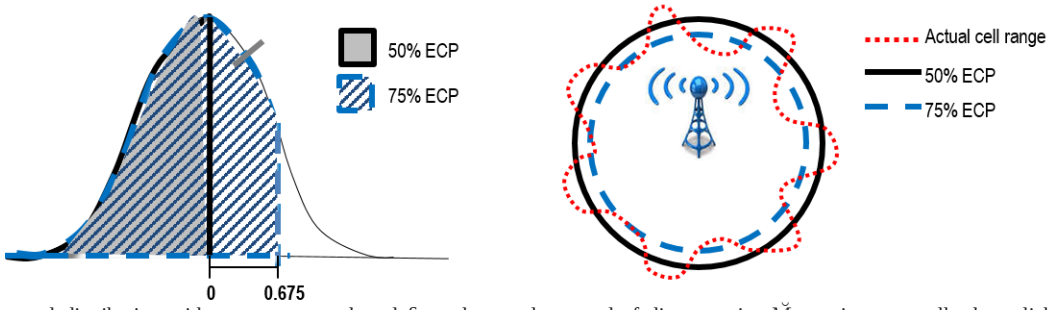

Fig. 4. Left: Log normal distribution with zero mean used to define adequate large scale fading margin, $\breve{M}_f$, to improve cell edge reliability. Right: Actual cell contour fluctuates due to large scale fading (dotted random line). Deterministic cell contour ignoring the large scale fading variables (solid circle) results in 50% locations on the cell edge with received signal strength equal or better than target. Deterministic cell contour including large scale fading margin $\breve{M}_f$, obtained from the distribution on the left, results in 75% locations on the cell edge with, at least, required target received signal strength (dashed circle).

often represented using a log-normal distribution. The log-normal distribution's standard deviation depends on the area, frequency and size of obstructions; it is typically between 4dB and 12dB [29]. Figure 4 (left) depicts a normalised log-normal distribution with zero mean (standard deviation is set to 1). Traditionally, a fading margin ($\breve{M}_f$) is added to the target signal strength to account for the statistical fluctuation of the signal power, and thus, improve the reliability from 50% to 75%, for instance. In order to identify the adequate fading margin, firstly, the distribution in Figure 4 (left) is used, and a normalised margin of 0.675 is found to improve the reliability to 75%, with only 25% of the values falling above this value. Then, $\breve{M}_f$ is found by multiplying 0.675 by the standard deviation of the actual fading distribution (e.g., 8dB), consequently, $\breve{M}_f = 0.675 \cdot 8 = 5.4\text{dB}$. The improved-reliability target signal strength is thus, $-90 + 5.4 = -84.6\text{dBm}$ and the resulting cell contour is shown in a dashed line in Figure 4 (right). Thus, adding

the fading margin, $\breve{M}_f$, improves the cell edge coverage probability but reduces the cell range. Using Reudink's mapping between edge coverage probability and area coverage probability, and assuming a path loss exponent of 35.2dB per decade and a path loss constant of 137dB, then the area coverage probability that would result from such a design would be 90% reliability.

C. Traditional cell range calculation

The final outcome of the link budget is the maximum allowed path loss, or MAPL, which defines the maximum possible loss as a result of propagation loss that can exist between receiver and transmitter in such a way that the transmitter is on full power and the receiver achieves the required SINR, for the target ACP. Accordingly, the MAPL is the difference between the EiRP per sub-carrier ($\breve{P}$), affected by the design margins, and the target SINR at the cell edge ($\breve{\gamma}_{\mathrm{target}}$) as shown in Table II. In order to simplify the representation of MAPL, the effective power per sub-carrier ($\breve{T}$) will be calculated based on the EiRP per sub-carrier ($\breve{P}$) by adding all deterministic gains and subtracting all deterministic losses, thus, $\breve{T} = \breve{P} + \breve{M}_{G_{\mathrm{total}}} - \breve{M}_{B_{\mathrm{total}}}$, as shown in Table II. In reality, the MAPL ($\breve{L}_{\max}(\breve{A}_s, \breve{\mu})$) is a random variable affected by both variables: $\breve{A}_s$, for fading on serving cell and $\breve{\mu}$, for interference degradation. For the purpose of the link budget, a deterministic MAPL, conditioned on the fading variable modelled via the margin $\breve{M}_f$ and the interference degradation variable modelled via the margin $\breve{M}_\mu$, is computed based on the power balance of all deterministic parameters in the link budget, negated by a design margin ($\breve{M}_f + \breve{M}_\mu$). Accordingly, the deterministic MAPL, $\breve{L}_{\max}$, can be expressed as follows in dB, which matches the link budget in Table II:

$$\breve{L}_{\max} = (\breve{P} + \breve{M}_{G_{\mathrm{total}}} - \breve{M}_{B_{\mathrm{total}}}) - (\breve{\gamma}_{\mathrm{target}} + \breve{\sigma}^2 + \breve{M}_f + \breve{M}_\mu) = (\breve{T} - \breve{\gamma}_{\mathrm{target}} - \breve{\sigma}^2) - (\breve{M}_f + \breve{M}_\mu) \tag{3}$$

Consequently the cell range is also a random variable, $R(A_s, \mu)$, and the deterministic maximum cell range can be derived as follows by equating (3) and (1) and solving for R to obtain the maximum possible cell range:

$$\log_{10} R_{\max} = \frac{\breve{L}_{\max} - \breve{K}}{-10\alpha} \tag{4}$$

D. Effect of fading and interference degradation margins

Figure 5 is used to depict the effect of the fading margin and the interference degradation margin on the cell range. The received signal strength ($\breve{S}$) is represented in dBm as a function of the log distance R in km. In this figure, the fading margin is the difference between the solid line corresponding to mean received power and that of the dashed blue line that guarantees 75% samples above the target value $\breve{S}_{\mathrm{target}_1}$. The fading margin is derived as explained in Section II-C and results in bringing the cell edge closer to the base station (from r_0 to r_1). The interference degradation margin accounts for SNR degradation due to the presence of neighbouring interfering cells. Since the thermal noise is constant, the SNR degradation is actually the degradation of the target received signal power ($\breve{S}_{\mathrm{target}}$). In other words, to maintain the target SNR in the presence of other cell interference, the target received signal power needs to be increased from $\breve{S}_{\mathrm{target}_1}$ to $\breve{S}_{\mathrm{target}_2}$. In Figure 5, $\breve{S}_{\mathrm{target}_1}$ represents the target received signal power for an isolated cell and $\breve{S}_{\mathrm{target}_2}$ represents the same in a multi-cell deployment scenario. The difference between $\breve{S}_{\mathrm{target}_1}$

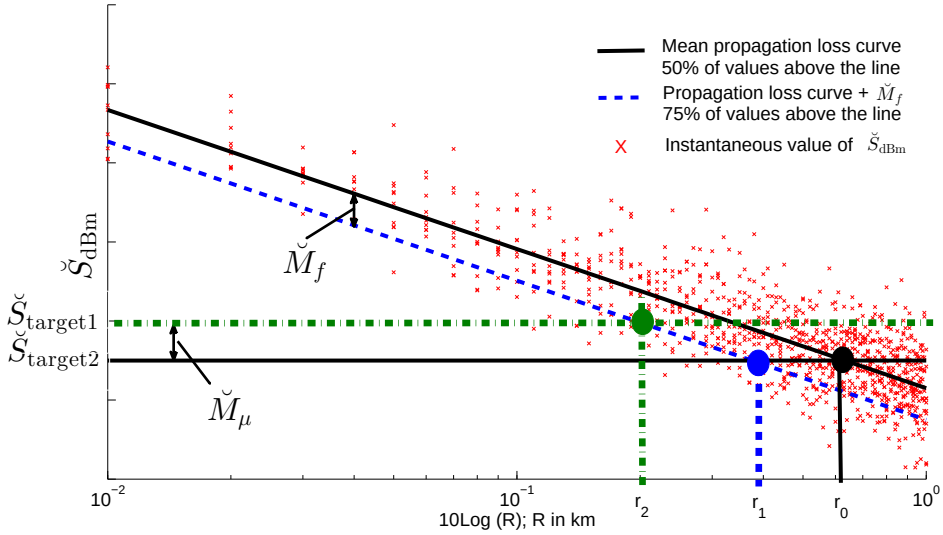

Fig. 5. Effect of large scale fading margin ($\breve{M}_f$) and interference degradation margin ($\breve{M}_\mu$) on the cell range. r_0, defined by the intersection of the $\breve{S}_{\mathrm{target}_1}$ line and the mean propagation curve, is the mean cell range without large scale fading considerations in an isolated cell scenario (black dot). r_1 is cell range as a result of including fading; it is defined as the intersection between the $\breve{S}_{\mathrm{target}_1}$ line and the propagation curve attenuated by a margin $\breve{M}_f$ (blue dot). r_2 is the effective cell range, when more that one cell reuse the same frequencies; it is the intersection between the $\breve{S}_{\mathrm{target}_2}$ line and the attenuated propagation curve (green dot).

and $\breve{S}_{\mathrm{target}_2}$ represents the interference degradation margin and depends on the level of activity or load in the network.

In reality, fading and interference degradation are variables governed mostly by the fading characteristics of serving and interfering cells. Traditionally, these variables have been accounted for, in dimensioning, through statistical margins ($\breve{M}_f$ and $\breve{M}_\mu$), derived from Monte Carlo simulations [31]–[33]. Fading distributions in cellular systems are well known and usage of log-normal distribution to represent large scale fading, or Rayleigh and Rice to represent small scale fading are commonly accepted. On the other hand, the interference degradation distribution in an LTE system has not been framed yet; the tradition, nevertheless, consists of adopting pragmatic margins inspired from UMTS link budgets.

This pragmatic assignment renders the traditional approach insensitive to LTE specific dynamics. As an outcome, the resulting design is often pessimistic, i.e., the network is over-dimensioned due to high setting of $\breve{M}_\mu$, thus additional cost is incurred with no added value. In Section III of this tutorial, we overcome this problem by first defining the interference margin as a function of cell loading and fading characteristics on channels from interfering cells. Accordingly, the statistical distribution of the interference degradation is derived, hence, enabling the appropriate setting of $\breve{M}_\mu$ in the link budget. This leads the way to a statistical link budget analysis, which, finds the distribution of the cell range as a function of fading and interference from other cells.

E. LTE/ LTE-A link budget

The principle and objective of LBA remain the same in all cellular generations. Essentially, it is a power budget exercise that targets the cell edge users to find the maximum allowed path loss. However, parameter interpretation and points of reference do vary significantly, resulting in a technology specific LBA for each of the 2G, 3G, and 4G networks. An LBA comparison between the three cellular generations is provided in Section II-E.1, and a discussion on the impact of LTE-A features impact on the LBA is presented in Section II-E.2.

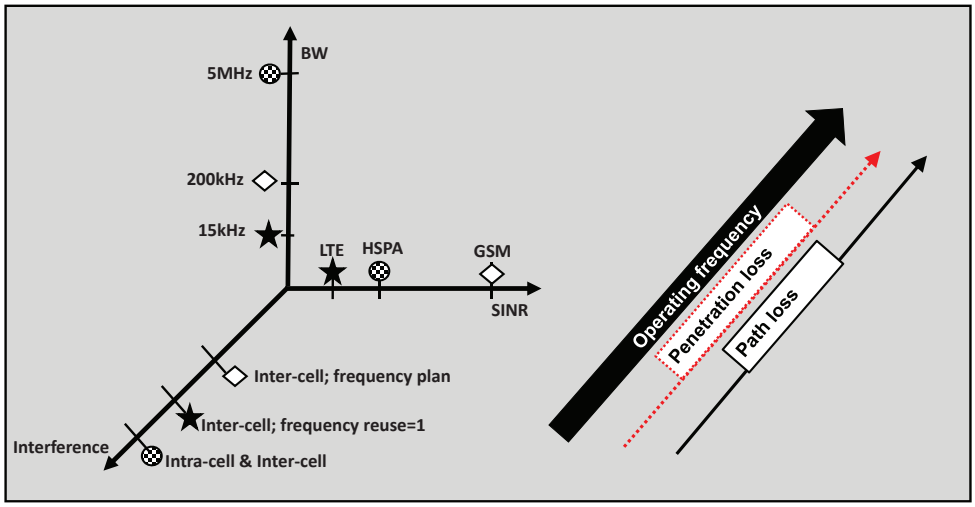

Fig. 6. The figure on the left represents a comparative diagram for 2G, 3G, and 4G, showing three critical LBA parameters that are radio access technology specific. It should be noted that, related to LTE, the 15kHz is the bandwidth per sub-channel; the total spectrum bandwidth can be up to 20MHz (without carrier aggregation). A reduced sub-channel spacing of 7.5kHz is also possible in LTE, e.g., the physical random access channel (PRACH). The figure on the right shows LBA parameters that depend on the operating frequency, which may differ among the three different cellular technologies.

1) LTE LBA in comparison with UMTS/HSPA and GSM: Key technology-related differences in GSM, UMTS/HSPA, and LTE link budget parameters are depicted in Figure 6 (left) and differences related to the operating frequency are shown in Figure 6 (right). The first technology-related difference concerns the channel bandwidth. UMTS, for instance, is based on a 5MHz channel bandwidth; whereas LTE uses 15kHz and 7.5kHz narrow sub-channels. This difference affects the thermal noise power and consequently the noise floor. Moreover, the target SINR in LTE has been alleviated due to various radio access design characteristics and advances; accordingly, a lower SINR can achieve the same data rate as in HSPA [6]. Sources of interference, however, differ fundamentally among radio technologies. GSM is a frequency division multiple access technology, hence intra-cell signals are orthogonal; however, frequencies/channels are often reused, within a network, which generates some level of inter-cell interference. UMTS is a spread spectrum radio technology, i.e., users share the same bandwidth and are only separated by spreading and scrambling codes. In this case, the SINR calculation includes two interference components: intra-cell interference and inter-cell interference, in addition to the thermal noise. The interference contribution is thus directly related to the channels' fading and the serving and neighbouring cells' load, which are relative to the pole capacity. On the other hand, LTE is an OFDMA technology, in which intra-cell interference is minimal while inter-cell interference is dependent on interfering cells' activities (i.e., cell load) and fading on each corresponding received signal. In this case, inter-cell interference is related to the probability of neighbouring cells reusing the same sub-channels simultaneously. Hence, scheduling schemes matter greatly in estimating this probability, and basically, higher cell loads would lead to higher chances of sub-channel reuse. The cell load in LTE is relative to the percentage of used resources; whereas in UMTS/HSPA, it is related to the pole capacity. Inter-cell and intra-cell interference affect the SINR ratio variation and, thus, need to be captured in the corresponding interference margin variable in the link budget analysis as shown in Figure 3. A statistical model of LTE interference margin is utilised in this tutorial to highlight the need for further research in the domain of LTE analytical dimensioning.

The measurement reference point is another major difference between UMTS/HSPA and LTE. UMTS is dimensioned in view of the received signal code power (RSCP) over the 5MHz bandwidth; whereas, LTE is concerned with the reference signal received

power (RSRP) over a sub-channel bandwidth of 15kHz. Other major differences between UMTS and LTE are related to the operating central frequency such as: penetration loss and path loss model, as highlighted in Figure 6 (right).

2) LTE/LTE-A advanced features in LBA: The link budget in Table II captures the LTE specific parameters, as explained above, for the basic LTE deployment. Nonetheless, there are optional advanced LTE features, such as inter-cell interference coordination and coordinate multi-point transmission/reception (CoMP), that should also be accounted for in the dimensioning exercise. Inter-cell interference coordination (ICIC) was first introduced in LTE release 9, enabled by the exchange of load and interference information over the X2 interface (LTE interface between eNBs). Accordingly, eNBs use this information in the scheduling algorithm to avoid allocating resources, that are highly used in neighbouring cells, to cell edge users that are vulnerable to interference. With the emergence of heterogeneous networks in LTE-A, enhanced ICIC (eICIC) was defined in release 10, in which almost blank sub-frames (ABS) are used on the macro-layer to reduce downlink interference on UEs associated with small cells. LTE release 11 includes further enhanced ICIC (feICIC), which aims at handling interference by the UE through inter-cell interference cancellation for control signals, enabling further small cell range extension. xICIC is essentially based on shared information among neighbouring cells, which is used in the resource scheduling algorithm to avoid ICI [34]. Evidently, ICIC in all its forms affects the level of ICI, as well as the network coverage and capacity. Authors in [35] demonstrate increase in cell edge users throughput as well as cell overall throughput with xICIC. Authors in [19] propose an analytical model for ICI for different scheduling algorithms such as greedy, proportional fair and round robin. From a coverage dimensioning perspective, different ICIC algorithms would generate different levels of inter-cell and inter-layer (between macro-cells and small cells) interference, and should be captured in the interference degradation estimation in the LBA. Moreover, the capacity dimensioning should account for the ICIC scheme implemented, such as the presence of ABS [35].

CoMP would certainly affect the coverage dimensioning, since it can provide diversity gains that can directly boost the SINR levels. Also, capacity resources from all cells in the CoMP cluster would be used simultaneously for one user; this should be accounted for in the capacity dimensioning. On the other hand, there are many forms of uplink and downlink CoMP which would result is variable gains and consume different resources from cells in the CoMP cluster. It would be an interesting future area of research to consider the interplay between cellular network planning/deployment and CoMP enhancements.

LTE-A is an evolution of basic LTE with improved ICIC and new features such as carrier aggregation and heterogeneous networks. Carrier aggregation is introduced in release 10 of LTE and further extended in release 11. It basically consists of equipping a cell with more than one carrier components (total maximum bandwidth up to 100MHz) with joint scheduling, hence reaching users with higher data rates. These carrier components may be in different parts of the spectrum, hence, would have different frequency-related LBA parameters (see Figure 6 (right)). Consequently, the structure of the LBA remains as in Table II, however, different operating frequencies would result in different link budgets. Moreover, it is critical to capture the scheduling of different components in the ICI modelling and in the capacity dimensioning. For example, in [36], a distributed interference coordination scheme for femto-cells

(cells with very low transmit power, often used for indoor coverage) with carrier aggregation is proposed. Each femto-cell operates on all the carrier components of the network, initially, and then decides whether to maintain each of the carrier components based on local measurements. The proposed algorithm is shown to reduce the ICI, and consequently increase the SINR and the throughput. Therefore, the implementation of carrier aggregation will impact coverage and capacity network dimensions, and should be reflected in the ICI estimation; a key parameter affecting the SINR, hence the link budget and network throughput.

Heterogeneous networks are multi-layered, consisting of macro-cells and small-cells (low power cells). Small cells are mainly used for data offloading while the macro-cells provide the ubiquitous coverage; they may share part of, or all the spectrum, and they may have dedicated spectrum. In a dedicated spectrum deployment, each network layer is dimensioned separately using the described LBA with adjusted parameters for the small cells such as transmit power and propagation model. Otherwise, the SINR calculation should also account for inter-layer interference as part of the ICI, with possibly different cell loads on different layers; however, the LBA remains typically the same. Authors in [37], for instance, provide a simulation-based dimensioning approach for heterogeneous networks. The approach assumes an initial number of cells, and performs the cell association process with the objective of maximising the users' throughput. Then, a cell elimination procedure is initiated to find the minimum number of cells that would preserve the network metric. Authors in [38] look at a heterogeneous network employing carrier aggregation, and propose a two-dimensional interference coordination scheme combining power control and component carrier assignment; consequently network outage is reduced significantly compared to a scheme using power control only. In this tutorial, we emphasize the need to capture heterogeneous networks and carrier aggregation in the dimensioning process, which would affect coverage and capacity results. Moreover, heterogeneous networks with multi radio access technologies (multiRATs), a feature of the fifth cellular system generation (5G), are further discussed in Section VII-A.

III. Statistical Link Budget Analysis (SLBA)

The traditional LBA is thus rigid, mostly in the interference degradation margin definition, and has no bridging between the capacity and coverage dimensioning. The impact of channel fading and cell loading on the interference degradation could be easily captured through simulations, such as Monte Carlo, but that would compromise the essence of the link budget analysis being purely analytical and fast in generating dimensioning results. The usage of statistical margins in link budgets, to improve reliability with known channel fading distributions, is a common practice as detailed in Section II-D. The usage of interference degradation margin is however different; effect of ICI is tightly related to the technology, and results obtained from previous cellular generations cannot be directly applied to LTE. Moreover, due to the many different deployment scenarios of LTE, it is not practical to rely on tabulated simulation results for identifying a suitable M_μ. Thus, it is a critical milestone to be able to capture the effect of interference degradation in the absence of prior results and without the need of simulations. Accordingly, there is a need to develop a generic LBA approach that reacts to the actual fading characteristics of interfering channels and probability of interference. It is

also essential to feed back results from capacity analysis to the coverage dimensioning, and vice-versa, to obtain a balanced radio dimensioning design.

These issues are addressed in the statistical link budget analysis, a new concept for link budget analysis introduced in our previous work [39]. The objective is to find the cumulative effect of variables affecting the LBA in the form of a statistical cell range distribution; hence statistical link budget analysis. The link budget is essentially a coverage dimensioning tool; it is nevertheless, tailored in view of capacity and QoS constraints. Capacity is represented by the interference degradation μ which is a function of loading in neighbouring cells. Quality of service is firstly captured by the setting of the target SINR (γ_{target}), conventionally defined through link level simulations which map the desired link BER/BLER to a required SINR for a defined data rate under given channel models. In addition, edge and area coverage probabilities are also a measure of QoS.

The first subsection details the derivation of the interference degradation margin as a function of cell loading and channel fading from interfering neighbours. Next, the derivations of statistical distributions of the SINR, the interference degradation, the MAPL, and the cell range are presented in the context of LTE and compared to simulation results for validation.

A. Interference degradation in LTE

In the light of the discussion presented in Section II, the interference degradation, due to simultaneous co-channel activity in surrounding cells, is defined and derived in this subsection. The proposed system model assumes N three-sector sites where each sector is modelled as a hexagon of diameter R and the base station is located at the intersection of the three sectors. The cell edge user receives the required signal from the serving cell but also interference from the $N-1$ other sectors in the network. The inter-site distance (ISD) is $\sqrt{(}3)R$. Neighbouring cell (n) has a cell load η_n which is the percentage of the used resources (power or sub-carriers) in the cell, and should reflect the effective capacity demand from the subscribers covered by the given sector [6]. The actual cell loads, per cell, vary spatially and temporally in a live network. However, the RND is designed for the peak traffic; hence, the cell loads used reflect the highest levels predicted. To account for spatial and temporal variations in traffic and corresponding cell load, intelligent radio access schemes are proposed to redistribute traffic in such a way that maximises the number of cells that can be switched off, without degrading the network performance. Authors in [40], for instance, propose a planning methodology that identifies the ideal location of eNBs and corresponding on/off switching patterns to economise on energy while preserving the network's performance, under changing traffic conditions. Transmitted signals are subjected to distance-based path loss and generic fading, as in (2), and universal frequency planning is assumed. In order to capture the interference degradation or noise rise in LTE, we first derive the downlink budget of an isolated cell considering the SNR at the cell edge. Next, we derive the link budget for a cell surrounded by $N-1$ interfering cells, considering the SINR at the cell edge, and compare it to the isolated cell scenario to capture the effect of ICI.

In the case of an isolated cell, there are no other cells to interfere with the user's signal hence, at the cell edge, the SINR is equal

to the SNR (γ') which can be expressed as the ratio of the signal from the serving cell, S as in (2), and thermal noise power, σ^2:

$$\gamma' = \frac{S}{\sigma^2} = \frac{\frac{T \cdot A_s}{L_s}}{\sigma^2} \tag{5}$$

where T is the effective transmit power dedicated to the cell edge user, L_s is the mean path loss between the serving cell s and the cell edge user as in (1), and A_s is the fading gain component on the corresponding radio link. The link budget is designed to secure a target SINR (γ_{target}) at the cell edge; thus by equating the measured SNR to the target SINR we can find the maximum allowed path loss that would satisfy the condition. Accordingly, we replace the measured SNR (γ') with the target SINR (γ_{target}) in (5), and solve for $L'_{\max} = L_s$ such that $\gamma' = \gamma_{\text{target}}$, as follows:

$$L'_{\max} = \frac{T \cdot A_s}{\gamma_{\text{target}} \cdot \sigma^2} \tag{6}$$

In a realistic LTE deployment scenario, the serving cell would be surrounded by many other LTE cells sharing the same spectrum, thus, causing interference to each other. In this case, the target edge performance is measured through the SINR as follows, where η_n is the loading on neighbouring cell n and T is the transmit power per radio link, assumed the same for all cells in the network:

$$\gamma = \frac{S_s}{\sigma^2 + \sum\limits_{n=1, n\neq s}^{N} \eta_n \cdot S_n} = \frac{\frac{T \cdot A_s}{L_s}}{\sigma^2 + \sum\limits_{n=1, n\neq s}^{N} \eta_n \cdot \frac{T \cdot A_n}{L_n}} \tag{7}$$

In a similar manner as done for an isolated cell, the measured SINR (γ) is equated with the target SINR (γ_{target}) in (7), then we solve for $L_{\max} = L_s$ such that $\gamma = \gamma_{\text{target}}$, as follows:

$$L_{\max} = \frac{T \cdot A_s}{\gamma_{\text{target}} \cdot \left(\sigma^2 + \sum\limits_{n=1, n\neq s}^{N} \eta_n \cdot \frac{T \cdot A_n}{L_n}\right)} = \left(\frac{T \cdot A_s}{\gamma_{\text{target}} \cdot \sigma^2}\right) \cdot \left(\frac{\sigma^2}{\sigma^2 + \sum\limits_{n=1, n\neq s}^{N} \eta_n \cdot \frac{T \cdot A_n}{L_n}}\right) = \frac{L'_{\max}}{\mu} \tag{8}$$

Comparing (6) to (8), the effect of neighbouring cells interference results is an additional noise to the maximum allowed path loss, referred to as interference degradation, as defined below:

$$\frac{1}{\mu} = \frac{1}{1 + 1/\sigma^2 \sum\limits_{n=1, n\neq s}^{N} \eta_n \cdot T \cdot A_n \cdot L_n} = \frac{\sigma^2}{\sigma^2 + \sum\limits_{n=1, n\neq s}^{N} \eta_n S_n} \cdot \frac{S_s}{S_s} = \frac{\gamma}{\gamma'} \tag{9}$$

In an isolated cell scenario, μ would be unity, $\gamma = \gamma'$, and $L_{\max} = L'_{\max}$. In a realistic deployment, an additional loss is incurred due to ICI, dependant on the cell loading and fading, thus limiting the maximum path loss further where $L_{\max} = \frac{L'_{\max}}{\mu}$. Consequently, the maximum allowed path loss is a function of multiple random variables.

B. SINR: Statistical distribution

On the downlink, the SINR for the cell edge user served by cell s and interfered by $N-1$ cells is defined as in (7). The pertinent random variables are A_s, related to the serving cell fading characteristics, and A_n related to individual channel fading

characteristics of each neighbouring interfering cell. Consequently, the SINR is a random variable affected by the channel fading characteristics of the desired signal (A_s) as well as that of the neighbouring cells (A_n). SINR is the key quality target of the dimensioning exercise and is the most complex to capture mathematically. Nonetheless, a closed form for the SINR distribution assuming Rayleigh small scale fading on all channels concerned is possible as shown in this section.

We first assume Rayleigh fading with unity average fading power such that the probability distribution function of the variable A is $f_A(a) = e^{-a}$. Accordingly, the total power received from interfering cells (I) is the sum of $N-1$ independent random variables, thus the distribution of I is the result of the convolution of $N-1$ distributions.

$$I = \sum_{n=1, n\neq s}^{N} I_n = \sum_{n=1, n\neq s}^{N} \eta_n \cdot X_n \cdot A_n \tag{10}$$

where, s is the serving cell index, $I_n = \eta_n \cdot X_n \cdot A_n$, η_n being the loading on neighbouring cell n, A_n being the random variable characterising the fading on that cell, and $X_n = \frac{T}{L_n}$ is the received signal strength without fading nor loading coefficient. The PDF representing the variations of the received signal from one source of interference I_n is as follows, where $\lambda_n = E[I_n] = \eta_n \cdot X_n \cdot E[A_n]$ is the expected value of I_n:

$$f_{I_n}(i) = {}^{1}\!/_{\lambda_n} \cdot e^{-({}^{i}\!/_{\lambda_n})} \tag{11}$$

We use the moment generating function (MGF) approach to transform convolutions to multiplications. The $\mathrm{MGF}_{I_n}(x)$ of I_n is thus $\frac{1}{1-\lambda_n \cdot x}$ and the $\mathrm{MGF}_I(x)$ of I is the product of $N-1$ MGFs as shown below:

$$\mathrm{MGF}_I(x) = \prod_{n=1, n\neq s}^{N} \frac{1}{1-\lambda_n \cdot x} \tag{12}$$

Using partial fraction expansion, the $\mathrm{MGF}_I(x)$ can be expressed as follows:

$$\mathrm{MGF}_I(x) = \sum_{n=1, n\neq s}^{N} \frac{c_n}{1-\lambda_n \cdot x} \tag{13}$$

$$c_n = \prod_{k=1, k\neq n, k\neq s}^{N} \frac{1}{1-{}^{\lambda_k}\!/_{\lambda_n}} \tag{14}$$

Expressing the product as a weighted sum, the distribution of I can be derived by inverting $\mathrm{MGF}_I(x)$ as follows:

$$f_I(i) = \sum_{n=1, n\neq s}^{N} {}^{c_n}\!/_{\lambda_n} \cdot e^{-({}^{i}\!/_{\lambda_n})}; i \geq 0 \tag{15}$$

Let Y and Z be as follows, where A_s is the random variable characterising the fading on the serving cell:

$$Y = \sigma^2 + I \tag{16}$$

$$Z = \frac{A_s}{Y} \tag{17}$$

Then their respective distribution can be derived as follows, based on the distribution of I:

$$f_Y(y) = \sum_{n=1,n\neq s}^{N} {}^{c_n}/_{\lambda_n} \cdot e^{-({}^{y}/_{\lambda_n})} \cdot e^{{}^{\sigma^2}/_{\lambda_n}}; y \geq \sigma^2 \quad (18)$$

$$f_Z(z) = \int_{\sigma^2}^{\infty} y \cdot f_A(yz) \cdot f_Y(y) dy \quad (19)$$

Finally, the SINR (γ) can be expressed as a function of Z such that $\gamma = X_s \cdot Z$, where $X_s = \frac{T}{L_s}$ is the received signal from the serving cell without fading consideration, and the corresponding distribution is as follows:

$$\begin{aligned} f_\Gamma(\gamma) &= \frac{1}{X_s} \cdot f_Z\left(\frac{\gamma}{X_s}\right) \\ &= e^{b_1\gamma} \sum_{n=1,n\neq s}^{N} \frac{c_n}{\lambda_n} \left(\frac{b_1}{b_2\gamma + 1/\lambda_n} + \frac{b_2}{(b_2\gamma + 1/\lambda_n)^2} \right) \end{aligned} \quad (20)$$

where $b_1 = \sigma^2 \cdot L_s$ and $b_2 = L_s$. It should be noted that at this stage a closed form expression for the SINR distribution assuming a composite fading distribution, that jointly captures large and small scale fading, is still not available.

C. Interference degradation: Statistical distribution

In the link budget, the capacity aspect is represented by the interference degradation as derived in Section III-A and represented in (9). The interference degradation (μ) measured by a cell edge user is thus a random variable affected by the channel fading characteristics of the neighbouring cells (A_n) considering the corresponding loading factor (η_n). The distribution of received interference from all cells (I), as defined in (10) in Section III-B, is found to follow $f_I(i)$ as in (15). Since $\mu = \frac{I+\sigma^2}{\sigma^2}$, the distribution of the interference degradation as a function of $f_I(i)$ can be expressed as follows:

$$f_M(\mu) = \sigma^2 \cdot f_I(\sigma^2(\mu - 1)) \quad (21)$$

Under Rayleigh fading, $f_M(\mu)$ can be derived as follows (see Figure 7 (a) for comparison with Monte Carlo simulations):

$$f_M(\mu) = \sigma^2 \cdot \sum_{n=1,n\neq s}^{N} \frac{c_n}{\lambda_n} e^{-\frac{\sigma^2(\mu-1)}{\lambda_n}} \quad (22)$$

To find the distribution $f_M(\mu)$ under composite fading, we approximate the PDF $f_A(a)$ of all A_n with a gamma distribution with shaping parameter m_n and inverse scaling parameter k_n [41]. Then, I_n also follows a gamma distribution with shaping parameter m_n and inverse scaling parameter ζ_n as defined below, resulting in $f_{I_n}(i)$, as in (24), where $g()$ represents the gamma function.

$$\zeta_n = \frac{\eta_n \cdot T \cdot k_n}{L_n} \quad (23)$$

$$f_{I_n}(i) = \frac{\zeta_n^{m_n}}{g(m_n)} i^{m_n - 1} e^{-\zeta_n i} \quad (24)$$

We assume that all ζ_n are positive distinct real numbers and impose the constraint that the m_n's are positive integers, not necessarily distinct. Each I_n is therefore the sum of m_n independent exponential random variables with mean $\frac{1}{\zeta_n}$. The moment generating function of $I = \sum_{n=1,n\neq s}^{N} I_n$ can be expressed as a function of the moment generating function of I_n as follows:

$$\mathrm{MGF}_I(x) = \prod_{n=1,n\neq s}^{N} \mathrm{MGF}_{I_n}(x) = \prod_{n=1,n\neq s}^{N} \frac{\zeta_n^{m_n}}{(\zeta_n - x)^{m_n}} \tag{25}$$

Through the partial fraction expansion, the moment generating function of I can be expressed as follows:

$$\mathrm{MGF}_I(x) = \sum_{n=1,n\neq s}^{N} \sum_{j=1}^{m_n} \frac{c_{nj}}{(x-\zeta_n)^j} \tag{26}$$

$$c_{nj} = \prod_{j=1,j\neq n}^{n} \frac{\zeta_n}{(\zeta_n - \zeta_j)} \tag{27}$$

Consequently, the distribution of μ is obtained after some manipulations, as shown below:

$$f_M(\mu) = \sigma^2 \sum_{n=1,n\neq s}^{N} \sum_{j=1}^{m_n} \frac{(-1)^j c_{nj}}{(j-1)!} (\sigma^2)^{j-1} (\mu-1)^{j-1} e^{-\zeta_n \sigma^2 (\mu-1)} \tag{28}$$

D. MAPL: Statistical distribution

The first outcome of the link budget is the MAPL, denoted by $L_{\max}$, as shown in (3). It indicates the maximum loss limit between transmitter and receiver (at the cell boundary) beyond which the outage probability will increase above the target. MAPL is, in essence, a function of two variables: A_s, the fading on the wanted signal and μ; however, by adopting an adequate fading margin M_f, it can be expressed as a function of a single variable μ, as in (29), by replacing the variable A_s in (8) by the statistical margin M_f. In logarithmic scale, $\breve{L}_{\max}(\breve{\mu})$ can then be expressed as follows:

$$\breve{L}_{\max}(\breve{\mu}) = \breve{T} - (\breve{\gamma}'_{\mathrm{target}} + \breve{\sigma}^2 - \breve{M}_f - \breve{\mu}) = \breve{L}'_{\max} - \breve{\mu} \tag{29}$$

Thus, in linear form, $L_{\max}(\mu) = \frac{L'_{\max}}{\mu}$ (see(8)), where $L'_{\max}$ is the MAPL of an isolated cell conditioned on A_s modelled via M_f, $\breve{L}'_{\max} = \breve{T} - (\breve{\gamma}_{\mathrm{target}} + \breve{\sigma}^2 + \breve{M}_f)$, and the distribution of MAPL can be derived as a function of the distribution of the interference degradation μ as follows:

$$f_{L_{\max}}(l) = \frac{L'_{\max}}{l^2} f_M\left(\frac{L'_{\max}}{l}\right) \tag{30}$$

E. Cell range: Statistical distribution

The cell range is derived from the path loss equation and the MAPL value as detailed in Section II-A. The cell range equation in (4) is re-written here, solving for R, where $\breve{L}_{\max}$ is as in (29), $\breve{K}$ is the propagation constant, and α is the propagation exponent:

$$R = 10^{\left(\frac{\breve{L}_{\max} - \breve{K}}{-10\cdot\alpha}\right)} \tag{31}$$

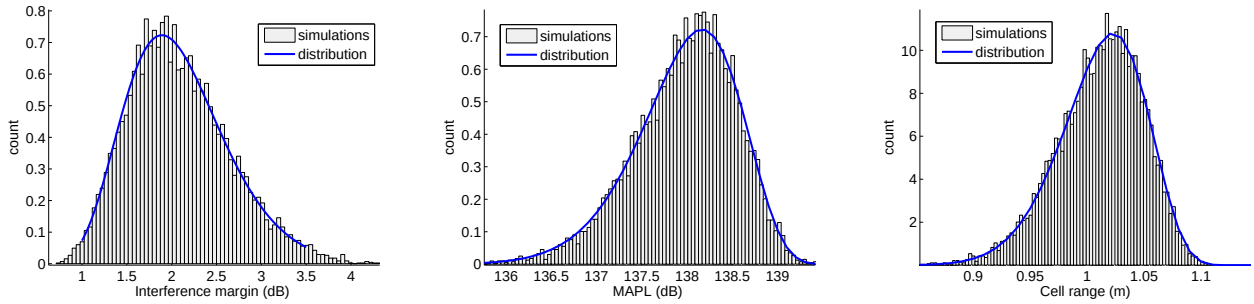

(a) Rayleigh fading: Interference margin distribution. (b) Rayleigh fading: MAPL distribution. (c) Rayleigh fading: Cell range distribution.

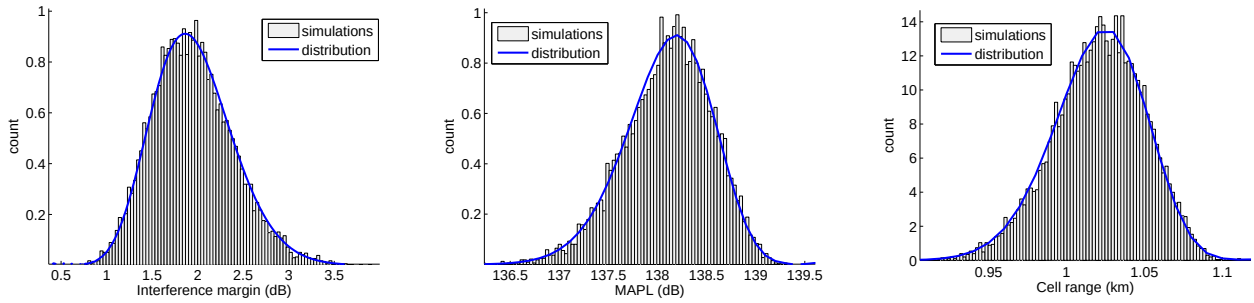

(d) Composite fading: Interference margin distribution. (e) Composite fading: MAPL distribution. (f) Composite fading: Cell range distribution.

Fig. 7. Comparison between derivations based on statistical distributions defined in Sections III-C, III-D, and III-E for interference degradation, MAPL, and cell range, respectively, and Monte Carlo simulations with 50% cell loading. Plots (a)-(c) are for Rayleigh fading channel model. Plots (d)-(f) are for composite fading channel model with shaping factor set to two.

Therefore, the distribution of the cell range, R, is directly derived from that of the MAPL ($L_{\max}$) as defined in (30) and can thus be expressed as follows:

$$f_R(r) = \frac{1}{K} \cdot \alpha \cdot r^{\alpha-1} \cdot f_{L_{\max}}\left(\frac{1}{K} \cdot r^{\alpha}\right) \tag{32}$$

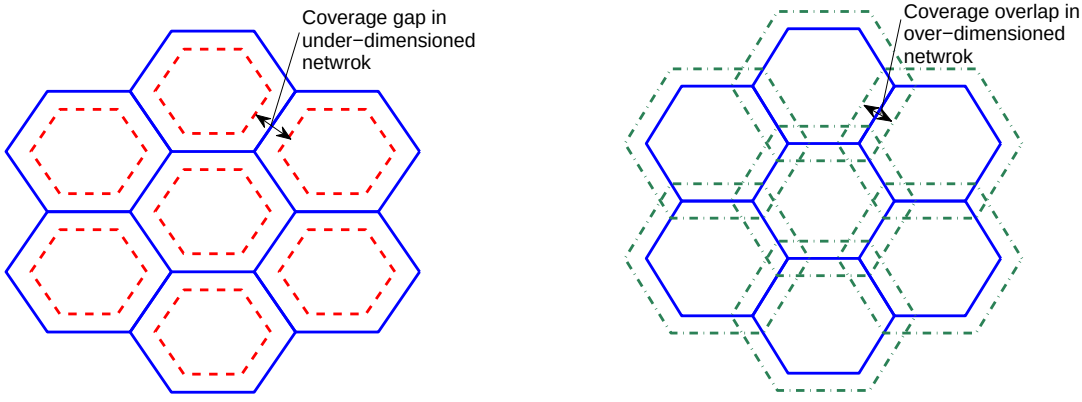

Fig. 8. The figure on the left side shows an under-dimensioned network; the figure on the right shows an over-dimensioned network. The dotted lines represent the actual cell boundaries based on received SINR, whereas the solid lines represent the Voronoi boundaries based on cell locations.

F. Verification with Monte Carlo simulations

The derived statistical distributions in Sections III-C, III-D, and III-E are validated by comparison with Monte Carlo simulations for both channel fading models: Rayleigh and composite fading. The results are presented in Figure 7 assuming 50% cell loading and shaping factor of two for the composite fading channel. The statistical distributions are found to match closely Monte Carlo

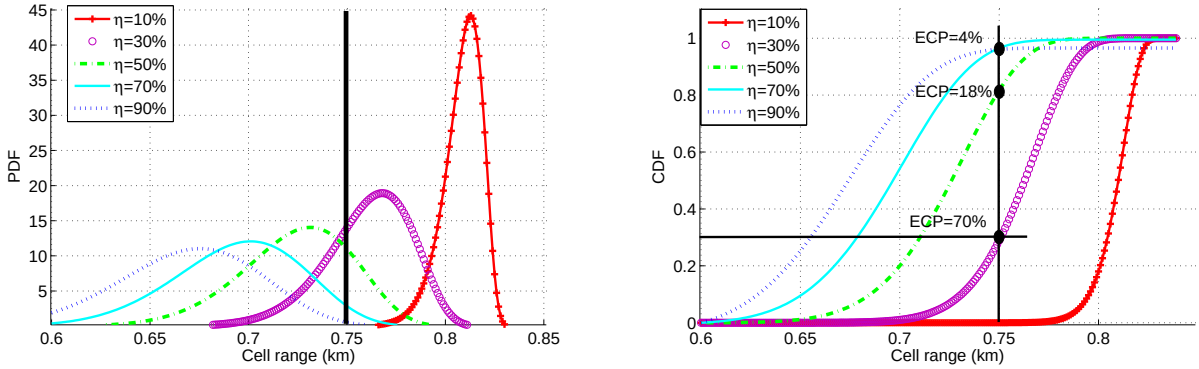

Left: PDF of effective cell range at different loadings. Right: CDF of effective cell range at different loadings.

Fig. 9. Effect of cell loading, η, on cell range distribution. The inter-site distance in all cases is 1.3km, thus the cell edge user is located at 0.75km from the eNB. Left: higher cell load results in wider standard deviation to the PDF curve, hence higher cell edge elasticity. Right: higher cell load results in shifting the CDF curve closer to the eNB and vice-versa, hence cell breathing.

results for both channel types and for three key dimensioning entities: interference degradation, MAPL, and cell range.

IV. Statistical Link Budget Analysis: Results and Insights

The statistical link budget analysis is a coverage dimensioning tool that computes the coverage cell range, based on presumed capacity (cell load). In parallel, capacity dimensioning is performed, to find the maximum capacity cell range, based on defined base station available capacity, and estimated traffic density. Ideally, both procedures should be tuned in such a way that the coverage cell range and capacity cell range are equal, hence creating a balanced design. If the coverage cell range is larger that the capacity cell range, the network is considered under-dimensioned as shown in Figure 8 (Left), in which there are coverage gaps between cells. On the other hand, when the coverage cell range is smaller, it would result in coverage overlap, as shown in Figure 8 (Right), which indicates that the network is over-dimensioned.

In order to explore the tradeoff characteristics inherent to LTE technology, we apply the cell range distribution derived in Section III-E to different network deployment scenarios. Three critical aspects of LTE dimensioning: cell breathing and elasticity, ISD effect, and transmit power effect, are revealed and described in Sections IV-A, IV-B, and IV-C, respectively.

A. Cell breathing and elasticity

Cell breathing is the trade-off relation between capacity (cell load) and coverage (cell range). The effect of cell loading is demonstrated in Figure 9 which presents the PDF and the cumulative distribution function (CDF) of the cell range. The inter-site distance considered is 1.3km, i.e., a cell range of 0.75km. Increasing the loading on the neighbouring cells moves the mean of the statistical cell radius towards smaller ranges (and vice-versa); a phenomenon referred to as *cell breathing*.

To demonstrate the tight dependency between capacity and coverage, we take a numerical example. Let us assume a subscriber density of D_S equal to 550 subscribers per km^2 and a maximum eNB (three-sectored) capacity of 2100 subscribers, then at 30% capacity cell load, one eNB can cater for $U = 630$ subscribers. The capacity cell range is first computed by calculating the area in which these subscribers are found using $U/D_S = 1.14\mathrm{km}^2$, consequently, the corresponding capacity cell range is equal to $0.76\mathrm{km}$. Next, statistical coverage analysis is performed. Referring to the results in Figure 10 (Left), the ISD at a cell load of 30% corresponding to a target edge coverage probability of 70% is 1.3km. This can be deduced looking at the point of intersection

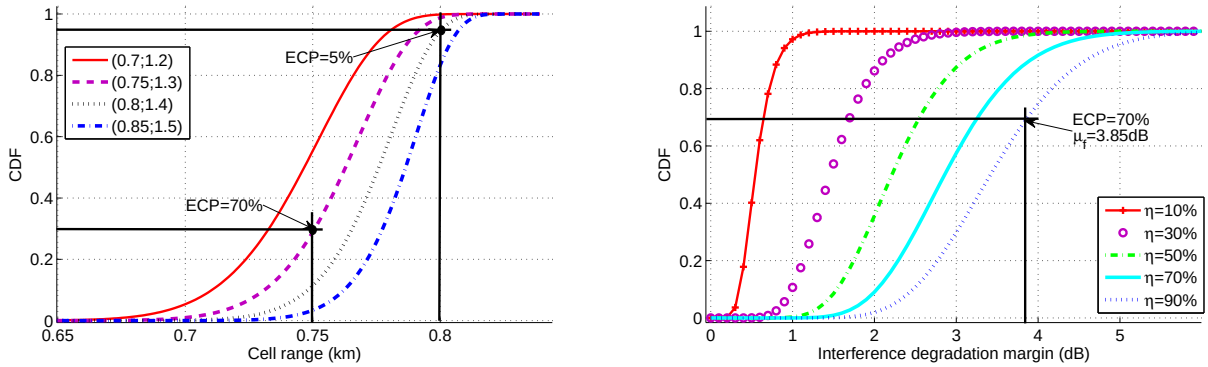

Left: Effect of inter-site distance on cell range distribution.

Right: CDF of cell range interference degradation margin.

Fig. 10. Left: CDF of cell range as a function of inter-site distance. The values in parenthesis in the legend correspond to (presumed cell range; inter-site distance). Cell load fixed at 30%. Changing the inter-site distance from 1.3km to 1.4km reduces edge coverage probability from 70% to 5%. Right: CDF of interference degradation margin as a function of cell load showing the effect of cell loading (10% to 90%). The inter-site distance in all cases is 1.3km.

between the 70% probability line and the 30% cell load curve in Figure 10 (Left). Thus the statistical coverage analysis, assuming 30% cell load, results in a cell range equal to 0.75km which is very close to the capacity cell range 0.76km and the design can be considered balanced between coverage, capacity and quality.

If, however, a quasi-full capacity cell load (90%) was used instead, i.e., $U = 1890$ subscribers, it would result in an interference degradation margin of 3.85dB with the same cell edge probability. This value can be deduced from Figure 10 (Right) by looking at the intersection of the 70% probability line and the 90% cell load curve. A fixed interference degradation margin of 3.85dB used in the link budget would lead to a coverage cell range of 0.54km. In the capacity analysis, the area covered by one eNB is first computed, 0.566km^2, consequently using $U = D_S \cdot 0.566 = 311$ subscribers, the capacity cell load can be found as the ratio $311/2100$ which is 15%, a much lower loading than assumed in the coverage analysis. This design is unbalanced, and since the actual cell load is less than the value assumed in the LBA, the eNBs are considered under-utilised, and the resulting network is over-dimensioned (see Figure 8 (Right)). Had we selected a low cell load, e.g., 10%, the design would have been unbalanced still, but with over-utilised eNBs, resulting in lower QoS and possible coverage gaps (see Figure 8 (Left)).

Moreover, higher cell loads result in wider cell range variations around the mean (refer to Figure 9 (Left)). This indicates that at high load, the aggregate effect of channel variations from the serving cell and the neighbouring cells amplifies the SINR fluctuations at the cell edge; this effect is referred to as *cell elasticity*. It is vital to correctly estimate the variation in the cell elasticity range as a result of loading when planning network parameters such as those related to handover, cell selection and congestion control. The cell edge ring, determined by the cell range elasticity, is more representative of the performance perceived by a cell edge user, when compared to the traditionally adopted margins that account for signal variations only. This is primarily true because the cell elasticity captures the aggregate effect of fluctuations of all channels affecting this user. Accordingly, the width of this hem can rightly be used in parameter settings, thus reducing the need for costly post network deployment optimisation.

B. Inter-site distance effect

The statistical cell range distribution is derived based on a predefined ISD, which is the presumed distance between two radio sites. The presumed cell range is calculated by dividing the presumed ISD by $\sqrt{3}$ (assuming hexagonal cells). The CDF of the

cell range, as an outcome of statistical dimensioning, indicates the probability of actually having a cell range less than or equal to the pre-selected value in a real cell. This probability, effectively reflects the outage probability of users at the cell edge. It should be noted that, in the context of LTE, an outage probability does not necessarily imply that the user would be out of coverage, nevertheless its achieved SINR, hence throughput, would deteriorate. In this section we study the relation between the presumed cell range, the resulting statistical cell range distribution, and the cell edge outage probability.

In Figure 10 (Left), the cell range CDF's under four different settings of ISD are drawn. Looking at the CDF curve corresponding to ISD=1.3km or 0.75km presumed cell range, we find that the statistical cell range varies, and its probability of being equal to or higher than 0.75km (the presumed cell range) is about 70% (i.e., cell edge outage probability 30%). This probability reduces though to 5% (i.e., cell edge outage probability 95%) when the ISD increases to 1.4km, as indicated by the probability of the effective cell range being equal to or higher than 0.8km (corresponding presumed cell range). It is, thus, of major importance to tune the ISD to the statistical cell range and, consequently, find the most adequate distance between radio sites that would reduce the performance degradation at cell borders. The importance is further amplified, in the case of LTE, since a mere 100 meters increase in the ISD would degrade the cell edge performance below acceptable levels.

C. Transmit power effect

Next, we explore the trade-off between total transmit power (P' in Table II), which is identically set in serving and neighbouring cells, and the statistical cell range. Increasing the transmit power of the wanted signal, naturally, boosts the received signal; however, the effect of increasing the transmit power of interfering neighbours, simultaneously, leads to a counter effect that needs to be analysed. The analysis is conducted under two scenarios: macro-cell (cell range of 1km) and small cell (cell range of 0.5km).

Firstly, an ISD of 1.732km (cell range of 1km) is fixed for three loads in neighbouring interfering cells (η): 10%, 50%, and 100% (Figure 11). For each of the scenarios, different total transmit power settings are considered and the resulting cell range distributions derived. First, analysing the effect of cell load on the cell range for three total transmit power settings: 31.8W, 39.8W, and 47.8W, in Figure 11 (a) and (b), it can be seen that higher cell loads reduce the impact of additional power on the cell range. Increasing the power from 31.8W to 47.8W enhances the cell range by 131m in the 10% cell load scenario and only 113m in the 100% cell scenario. This indicates that, higher cell loads result in higher ICI, which takes a leading role as an interference source in the SINR ratio, thus bringing it closer to signal to interference ratio (SIR). On the other hand, lower cell loads result in reduced ICI, leaving the thermal noise as the leading source on interference and bringing the SINR closer SNR. In Figure 11 (c), transmit power is increased to the point where, further augmentations have no effect on the cell range (case of 200W and 250W).

A case study on small cells deployment (ISD=0.866km) is then presented. In this case, the effect of transmit power is visible with a realistic transmit power range of 20dBm to 40dBm. Firstly, the effect of total transmit power on SNR/SINR average values is shown in Figure 12(a). As expected, SNR improves linearly with increased power, however SINR initially improves until it reaches saturation where the effect of ICI becomes much more important than thermal noise and SINR approaches SIR. In the

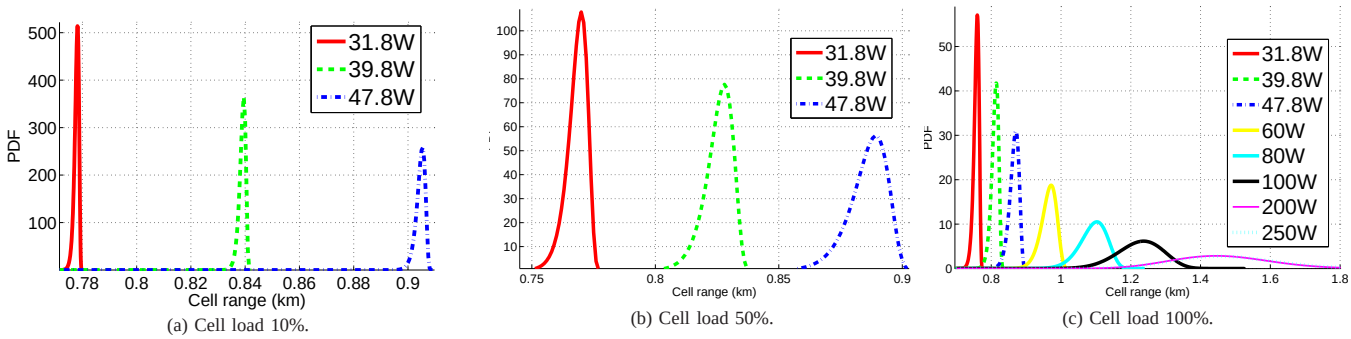

(a) Cell load 10%. (b) Cell load 50%. (c) Cell load 100%.

Fig. 11. Cell range distribution as a function of cell load and total transmit power. Cell load set to 10% (a), cell load set to 50% (b), and cell load set to 100% (c).

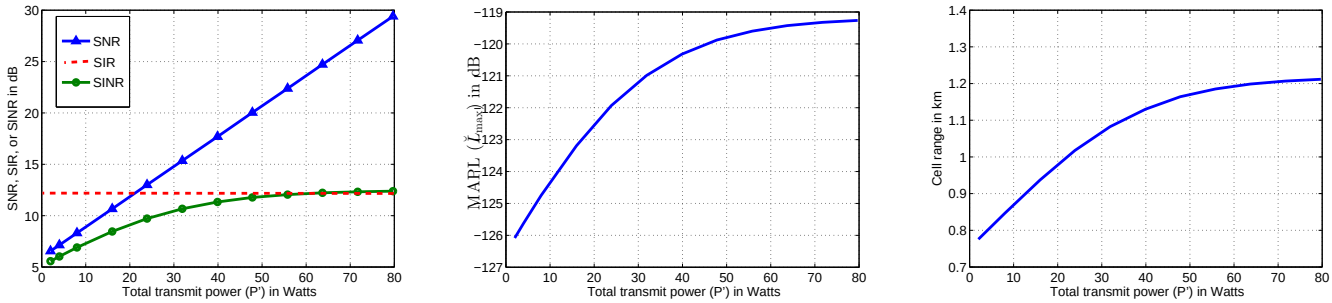

(a) SNR, SIR, or SINR as function of total transmit power. (b) MAPL as function of total transmit power. (c) Cell range as function of total transmit power.

Fig. 12. Effect of total transmit power on SNR, SINR, MAPL and cell range in a small cell scenario.

case of SIR, the power cancels out from numerator and denominator thus increasing power has no effect at all. Next, the effect of the total transmit power on the average MAPL and cell range is shown in Figures 12(b) and (c), respectively. Clearly, increasing the power beyond 30dBm has minimal gain on the cell range which approaches saturation after this inflection point, following the behaviour of SINR.

This relation between total transmit power (P'), capacity (η), quality (SINR), and coverage (cell range) is key to planning small cells. Small cells are a prime enabler to future cellular generations, owing to their improved area spectral efficiency. Due to their limited geographical footprint, small cells' design has a wide range of solutions varying from noise limited (when SINR is closer to SNR) to interference limited (when SINR is closer to SIR), thus it is very useful to find an efficient power setting that maximises the cell range with minimum ICI.

V. Iterative Statistical Analysis of LTE Dimensioning

In Section III we have described the statistical approach for interference modelling in an LTE network which lead to the derivation of statistical distributions of key dimensioning entities, namely, SINR, interference degradation, maximum allowed path loss and cell range. The causal relations between capacity, coverage and quality that have been drawn, highlight the need for accurate considerations of capacity demand in the link budget analysis, and uncover severe performance degradation that may result from pragmatic assumptions. Thus, the RND process cannot be solved solely with the LBA; issues, such as capacity and coverage balancing, require recursive link budget analysis to coordinate among conflicting requirements. Accordingly, an iterative approach is needed to yield a tuned downlink design in ISD selection and network parameter selection, as detailed in Section V-A. Nonetheless,

a complete RND exercise should find the balance between the downlink design and the uplink design; otherwise, it would result in coverage gaps as explained in Section V-B.

A. Iterative downlink dimensioning

In this section, we highlight the importance of iterative link budget analysis using the algorithm shown in Figure 13. The process starts by setting input parameters that are deterministic and user defined. A cell load η_A (typically 50%) is assumed and a pragmatic interference degradation margin is associated with it (typically 3dB). Then, the traditional link budget (see Table II) is used to find an approximate corresponding cell range r_A. Then, the inner loop is initiated which attempts to find the best ISD that would provide the required ECP ($\mathrm{ECP}_{\mathrm{target}}$). This is done using the SLBA, to derive the cell range distribution, and consequently, calculate the safe cell range r_S that satisfies the ECP and its corresponding ISD. Using SLBA to find the cell range distribution, through one iteration only, is not guaranteed to yield the required ECP; it is the case of when r_S is less than r_A. On the other hand, if r_S is greater than r_A, the design would be pessimistic, leading to over-dimensioning at a redundant extra cost.

When the difference between r_A and r_S is below a user defined target Δ_R, the inner loop reaches convergence, upon which the capacity analysis is initiated. Through the capacity analysis, the cell load based on the cell range r_S is obtained, denoted as η_C. If the difference between the assumed cell load η_A and the capacity cell load η_C is within the user defined error margin Δ_L, then the outer loop has converged. Otherwise, it will iterate until the convergence target is reached, by modifying the assumed cell load each time. It should be noted that for each iteration of outer loop, the inner loop reiterates until convergence. Moreover, there is a user defined upper limit on the number of iterations per inner loop and per outer loop which would halt the process even if there is no convergence. Furthermore, additional constraints govern the process such as minimum and maximum permissible cell load. If the network is lightly loaded, the minimum cell load will be used even if $\eta_A > \eta_C$. However, if η_C is higher than the maximum allowed, the transmit power of the base station will be attenuated to limit the coverage, and meet the balance with capacity requirements.

The cell range that results from this iterative process is tuned to the network conditions defined in the input parameters and the design targets. The cell edge user would have a probability of receiving the target SINR equal to the edge coverage probability; not more nor less (see Figure 8).

B. Uplink dimensioning and balancing with downlink

A complete RND exercise should consider the uplink direction, in addition to the downlink, and find a balance between them. A cell that reaches a larger radius on the downlink compared to the uplink, or vice-versa, is considered unbalanced, and would result in undesirable performance. Figure 14 (Left) shows a network design based on downlink LBA but not matched by the uplink; the users in the dashed area have good reception from the serving cell but fail to establish uplink connections. Figure 14 (Right) shows the opposite case, in which users in the dashed area do not receive a signal from the serving cell, although their uplink signal would have been well received. The dashed area in both cases is considered a coverage gap and should be avoided in network

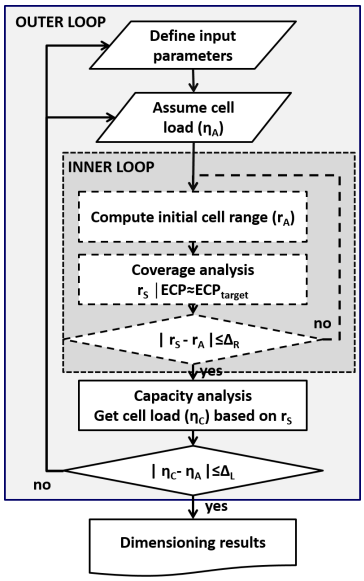

Fig. 13. SLBA-based process for LTE dimensioning. The outer loop finds the balance between the assumed cell load η_A and capacity cell load η_C. The inner loop finds the best inter-site distance that achieves an edge coverage probability (ECP) close to the target ECP ($\mathrm{ECP}_{\mathrm{target}}$).

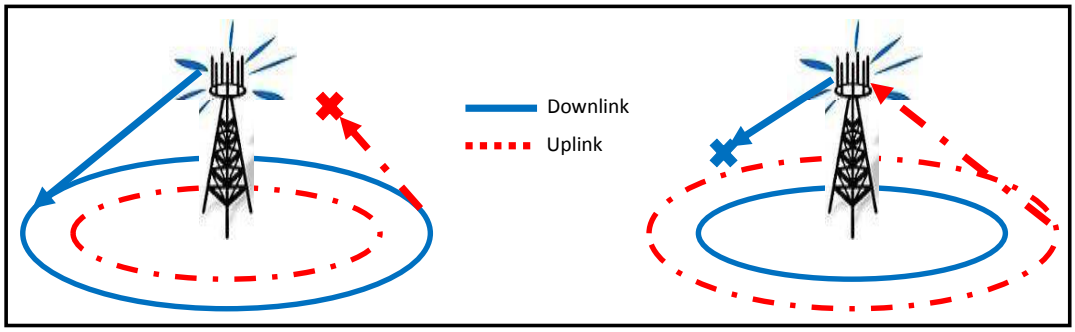

Fig. 14. The diagram on the left side shows a cell with better downlink coverage than the uplink. In this case the shaded area has good downlink reception but weak coverage. The right diagram shows a cell with better uplink coverage than downlink.

dimensioning and planning. Hence, it is essential to balance the uplink and downlink cell range in the dimensioning process. An uplink RND (i.e., iterative LBA) should be performed in parallel with the downlink RND, and the limiting link would be identified. The tuned cell range dictated by the limiting link should be adopted in the inter-site distance calculation and the eNB count. If the uplink cell range is limiting, the transmit power of the base station should be tuned down in the LBA in order for the downlink cell range to match the limiting uplink. On the other hand, if the downlink cell range in smaller, often the uplink LBA does not require modifications since the uplink power control would automatically tune down the uplink transmit power to match the limiting downlink cell range.

The uplink link budget is similar to the downlink shown in Table II with some differences as listed below:

- The total transmit power of a UE is lower than that of an eNB (e.g., 23dBm for class three UEs). The uplink budget should be dimensioned in view of the lowest performing UE expected in the network, which conforms with the 3GPP standards (3GPP TS 36.101).
- The transmit antenna gain is that of the UE and the receive antenna gain is that of the eNB (the inverse of the downlink budget). Normally, the UE antenna gain is considered 0dBi in the link budget.

- The eNB receive noise figure is often lower (e.g., 4-5dB [6]), i.e., better than the UE. The power amplifiers used in UEs are usually less performing than those in the eNBs, due to cost considerations; hence, UEs have higher noise figures.
- Interference degradation margin on the uplink is estimated to be typically lower than the downlink [6]). The uplink interference sources are active mobile UEs with low power and omnidirectional antennas; whereas the downlink interference sources are neighbouring eNBs at fixed locations with high power and directional antennas.

Consider a central serving cell surrounded by many cells reusing the same spectrum. Users in neighbouring cells may reuse the sub-channels allocated to a given user, and would cause interference to its uplink signal received at its serving cell. The uplink interference sources are then users that roam in the network, hence their location cannot be predicted. Moreover, features, such as fractional frequency reuse, inter-cell interference coordination, and scheduling, affect the level of interference generated by neighbouring users, and need to be captured in the derivations. Tabassum et al. have thoroughly researched this topic and have reached analytical modelling of the uplink inter-cell interference, taking into consideration composite fading and cell loading in the modelling. The authors have modelled uplink interference with channel based scheduling [42], proportional fair scheduling [43], with slow and fast power control mechanism [44], and with fractional frequency reuse [45], among other works.

Once the inter-cell interference is modelled, a similar statistical link budget analysis to that in Section III should be developed. Then the tuning between coverage and capacity constraints should be performed using an iterative method. The coverage design is based on the LBA, which includes the interference degradation, and is affected by the cell load, i.e., the users' distribution and profile and the scheduling algorithm. The capacity design takes as an input the cell range, and compares the generated throughput to the cell's capacity, based on the user's distribution and profile and the scheduling algorithm, to yield the effective cell load. Once the uplink RND is completed and tuned, it is compared to the downlink results; the limiting link would be the one that results in a smaller cell range and the other would be adjusted to match it.

VI. Pre-deployment Radio Network Planning: A Case study

In this section, we discuss how the two main steps in the pre-deployment phase of network planning can be combined (see Figure 1). This is done in a case study format, in which two approaches are considered for RND: the traditional RND and the SLBA-based RND. Next, the tool-based planning phase is undertaken, by feeding RND results to a network planning tool. Such a tool, supported by a digital terrain map, is capable of computing realistic propagation losses based on actual terrain elevation and clutter classification (refer to Figure 2). Also, the tool allows realistic representation of users and traffic, hence, it is used to generate realistic coverage and quality plots and outage statistics. The error margin between the RND and tool-based results is assessed for both approaches, as well as the gap between the QoS results obtained from the tool-based simulations and the pre-defined requirements.

There are various network planning tools in the market with similar features and capabilities such as Atoll by Forsk [46], Asset

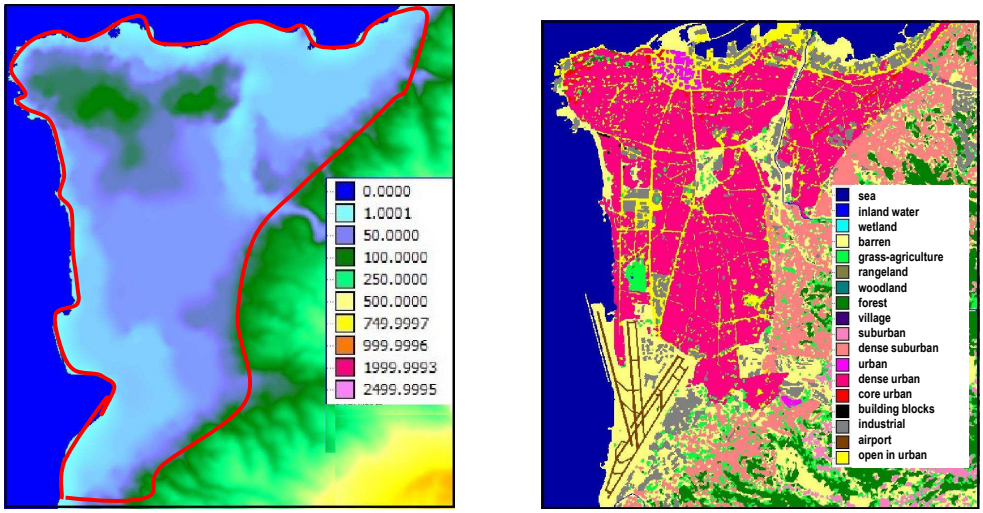

(a) Heights in meters in Ras Beirut.

(b) Clutter classification Ras Beirut.

Fig. 15. Area of Ras Beirut considered in the case study. Left side figure shows the heights in meters and the red line defines the focus area; the right side figure shows the clutter types.

by TEOCO [47], and Mentum Planet by InfoVista [48]. Mentum Planet 5.5.0.352 LTE FDD (frequency division duplex) is used in this case study. The tool is used together with a 20m resolution digital terrain map of greater Beirut and the focus area is selected to be Ras Beirut as shown in Figure 15. The tool computes propagation loss based on a digital terrain map and takes into consideration terrain height to analyse diffraction losses and uses clutter classification to adjust propagation losses according to additional clutter absorption loss.

The selected area is relatively flat, as shown in Figure 15(a), and covers a diverse range of varied clutter types ranging from core urban to suburban and forests (see Figure 15(b)). In a real life application, each clutter type would have a representative absorption loss (identified through field measurements) which would bias the propagation loss computation. In this case study, however, all clutter classes are assumed to have zero additional absorption loss, consequently propagation loss is mainly a factor of distance and terrain curvature. Clutter classification is also often used to gear the subscriber distribution and respective cellular network usage accordingly. For instance, it is normal to assume higher subscriber density in dense urban areas compared to villages; also it may be assumed that subscribers in industrial areas have higher usage to cellular services. However, in the case study presented, a uniform subscriber distribution is assumed throughout the area.

A. Analytical radio network dimensioning

To conduct the analytical RND exercise, the traditional and SLBA-based approaches are used, respectively, in Sections VI-A.1 and VI-A.2 to find the minimum number of eNBs needed to meet the pre-defined requirements. The RND parameters listed in Table II are adopted in both cases with other parameters as defined in Table III. The QoS parameters are the required SINR at the cell edge (γ_{target}) and the fading margin (M_f) which corresponds to the edge coverage probability. γ_{target} is defined based on link level simulations and depends on cell edge data rate requirement, but also on bit error rate or block error rate constraints, which are QoS related. In this case study, a typical value of $\breve{\gamma}_{\text{target}} = -2.1$dB is considered, corresponding to low spectral efficiency. $\breve{M}_f$, on the other hand, is defined using the log-normal distribution as described in Section II and, in this case study, 72.5% edge coverage

probability is required with a log-normal large scale fading standard deviation equal to 8.5dB. Using Reudink's relation between area and coverage probabilities [29], together with the propagation exponent in Table III, the target area coverage probability in this case is 88.2%. Capacity parameters listed in Table III have been introduced in Section IV, and the main propagation parameters are explained in Section II. The radio site area coefficient is a geometry-based coefficient, used in cellular network planning, to compute the area covered by a site knowing the range of one of its sectors assuming the shape of a sector is a hexagon and the range is its diameter. In the case of a three-sectored site the site area coefficient is 1.95.

TABLE III
RND CASE STUDY NETWORK PARAMETERS.

Capacity Parameters	**Unit**	**Value**
Subscriber density	$\mathrm{sub/km^2}$	550
Sector capacity	Mbps	35
Subscriber usage	kbps	50
Propagation Parameters	**Unit**	**Value**
Propagation exponent	dB/decade	35.2
Propagation constant	dB	-137
Site area coefficient		1.95

1) Traditional LTE dimensioning: In the traditional RND, a fading margin $\breve{M}_f = 5$ dB is used. The interference degradation is often accounted for through a power margin $\breve{M}_\mu$, typically 1-4dB; $\breve{M}_\mu$ =2dB is selected for this case study which is suitable for an urban environment. The major weakness of the traditional approach is the lack of analytical method to associate a given cell load with the appropriate $\breve{M}_\mu$; often a conservative value is adopted. Having defined all parameters, the link budget can be thus calculated and the dimensioning results are obtained as listed in Table II. The area covered by one radio site is $1.95 \cdot R^2$, where $R = 0.931$km, resulting in $1.8\mathrm{km}^2$ per eNB. The target area being $70\mathrm{km}^2$, requires $\lceil 70/1.8 \rceil = 39$ eNBs.

2) SLBA-based dimensioning: The same design assumptions and targets adopted in Section VI-A.1 are reused except for the interference degradation which is statistically estimated using the SLBA approach. Additional calibration parameters are listed in Table IV. The accepted error on cell range is Δ_R which represents the maximum acceptable difference between the assumed cell range (r_A) and the safe cell range (r_S) (refer to Figure 13). As explained in Section V, the safe cell range is derived from the cell range distribution for a given edge coverage probability. The accepted error on cell load is Δ_L, also shown in Figure 13. This represents the acceptable difference between the assumed cell load, η_A, and the capacity cell load, η_C, deduced from the resulting safe cell range and corresponding cell coverage area. The attenuation step is only used in case of capacity limited designs, identified by a capacity cell load higher than the allowed maximum. In these scenarios, the downlink power is attenuated in steps to reduce the coverage and meet the capacity constraints. The attenuation step defines the amount of attenuation used in every iteration.

SLBA-based dimensioning results are summarized in Table V, which shows a larger tuned cell range and fewer eNBs compared to the traditional approach results in Section VI-A.1. It can also be seen that the resulting design is coverage limited since no

attenuation is required. The actual cell edge probability is an outcome of the SLBA-based algorithm and, is deduced from the tuned cell range distribution; it is the probability of the cell range being equal or greater than the tuned cell range (1.026km).

TABLE IV
SLBA-BASED RND: ADDITIONAL CALIBRATION PARAMETERS.

Calibration parameters	**Unit**	**Value**
Accepted error on cell range, Δ_R (Inner loop)	m	10
Accepted error on cell load, Δ_L (Outer loop)	%	1
Attenuation step	dB	0.5

TABLE V
SLBA-BASED RND RESULTS.

Results	**Unit**	**Value**
Number of iterations	total	10
Run time	sec	41.7
Tuned cell range	km	1.026
Cell load	%	54.75
Actual edge coverage probability	%	73
Required attenuation	dB	0
Number of required eNB	eNB	32

B. Tool-based radio network planning

The second level of network planning consists of using the outcome of the first step (i.e., RND), and adding another layer of complexity such as actual terrain and realistic maps. Thus the outcome would be closer to real propagation and capacity demand in the given area. Consequently, the dimensioning results obtained in Sections VI-A.1 and VI-A.2 are used as an input to the automatic cell planning (ACP) tool. The ACP automatically generates identical and equidistant radio sites to fill up a user defined area based on the cell range obtained.

LTE analysis of both scenarios is conducted in the ACP tool and the results are compared. For each scenario, two coverage plots are generated: downlink SINR and downlink coverage. The downlink SINR plot represents the average downlink SINR per pixel, taking into account the received signal strength with power control, the thermal noise, and ICI. The downlink coverage is a binary plot, which gives a dark blue colour if at least one of the defined LTE modulation and coding schemes (MCS) is achievable, according to the downlink SINR.

Furthermore, capacity analysis is performed in the commercial tool using Monte Carlo simulations for each of the two scenarios. Monte Carlo simulations take as an input the coverage maps created, in addition to user defined subscriber and traffic maps. Accordingly, several iterations are run and, in each iteration, subscribers are spread randomly using Poisson distribution and densities defined in the traffic maps. For each subscriber, in each iteration, the possibility of a connection is assessed and in case of failure, the reason is identified. Iterations are repeated until the results converge to a user defined target. Thus, Monte Carlo

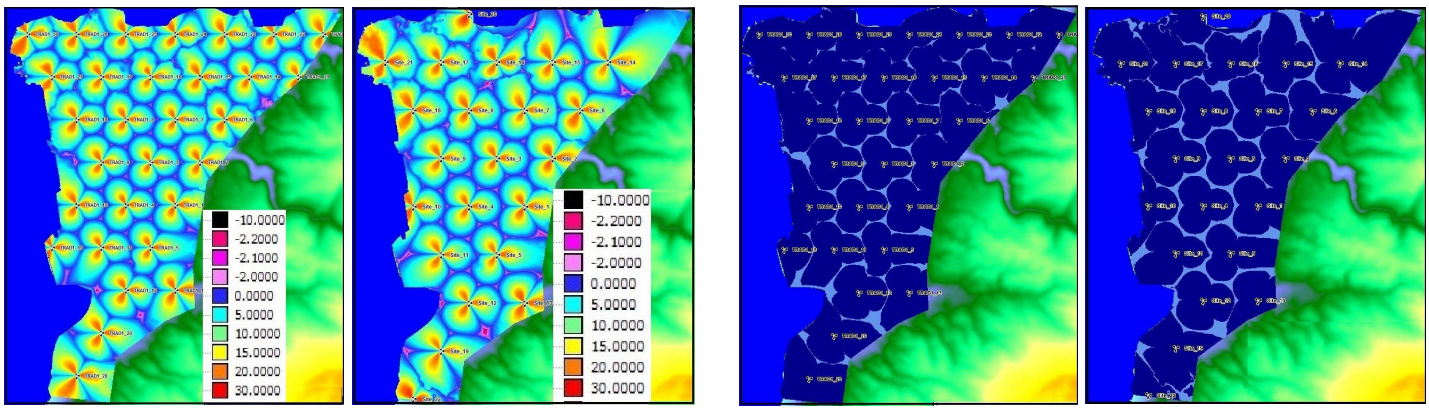

(a) SINR: Traditional scenario. (b) SINR: SLBA-based scenario. (c) Downlink coverage: Traditional scenario. (d) Downlink coverage: SLBA-based scenario.

Fig. 16. Plots (a) and (b) show the SINR (dB) plots for the traditional and SLBA-based scenarios, respectively, while indicating the radio site locations. Plots (c) and (d) show the downlink coverage plots from each scenario. The dark blue indicates coverage, i.e., at least one of the listed MCS is achievable according to the downlink SINR; otherwise the pixel is considered not covered and is marked with light blue colour.

simulations result in blocking probability, i.e., percentage of successful connections, and cell load per cell. This is clearly a QoS key indicator of performance perceived by the users.

1) Commercial tool results for traditional dimensioning: The ACP procedure, using traditional RND output, results in 30 eNBs and the corresponding coverage plots are shown in Figures 16(a) and (c) for downlink SINR and downlink coverage, respectively. Moreover, the downlink coverage results are summarised in Table VI. It is worth noting that the ACP tool results in nine less sites compared to the RND results in Section VI-A.1. There are three main reasons for this discrepancy: the approximation taken in the area coefficient, the form of the focus area, and the terrain elevation. In RND, a cell is approximated with a hexagon and the area covered by a cell is computed using the area coefficient; in ACP however, the shape of the cell coverage depends on the terrain, clutter and antenna pattern. Also, in the RND exercise, it is assumed that the target area is composed of hexagons with identical dimensions for all cells, i.e., all cells are completely contained in the target area, and no part of that area is left uncovered. In ACP however, the user defined target area does not comply with RND assumptions and, thus, some parts of the area are not well covered. In a realistic radio network planning exercise, the ACP results are further optimised to insure that the target area is completely covered adequately.

The area coverage probability obtained is 94% (Table VI) which is higher than the target value of 88.2%. The cell load results from the Monte Carlo simulations are listed in Table VII and success rate results are listed in Table VIII. The average downlink cell load is 40.85% and the success rate is 91.1%.

TABLE VI
TOOL DOWNLINK COVERAGE RESULTS.

	Traditional	SLBA-based
Covered area (km^2)	62.4	59.7
Total area (km^2)	66.4	66.4
Area coverage probability	94.0%	89.9%

2) Commercial tool results for SLBA-based dimensioning: The ACP procedure, using SLBA-based RND output, results in 22 eNBs and the corresponding coverage plots are shown in Figures 16(b) and (d) for downlink SINR and downlink coverage,

TABLE VII
TOOL DOWNLINK CELL LOAD RESULTS.

Downlink cell load	Number of cells	Number of cells
η_x	Traditional	SLBA-based
$\eta_x < 30\%$	17	8
$30\% \leq \eta_x < 40\%$	20	5
$40\% \leq \eta_x < 50\%$	34	12
$\eta_x \geq 50\%$	19	41
Average cell load	$\sum_{x=1}^{90} \frac{\eta_x}{90}$	$\sum_{x=1}^{66} \frac{\eta_x}{66}$
$\overline{\eta}$	40.85%	53.1%

TABLE VIII
TOOL MONTE CARLO SIMULATION RESULTS.

Monte Carlo results	Traditional	SLBA-based
Number of subscribers spread	3558	3576
Number of successes	3270	2945
Percentage success	91.1%	82.4%

respectively. The downlink coverage results are summarised in Table VI. In this scenario as well, the ACP tool results in ten less eNBs compared to the RND results in Section VI-A.2 for the same reasons discussed above.

The area coverage probability obtained is 89.9% (Table VI) which is very close to the target value of 88.2%. The cell load results from the Monte Carlo simulations are listed in Table VII and success rate results in Table VIII. Results from the traditional scenario show better coverage performance since about 91.1% of the users have the required coverage performance, but also incurs higher number of eNBs and unnecessary higher capital and operational expenditure. From a dimensioning point of view, the SLBA-based RND gives better performance since the results obtained are closer to the design target, thus, provides an economical solution that matches the deployment targets. Moreover, an average cell load is computed in Table VII which is the sum of the loads of all cells (90 in the traditional case and 66 in the SLBA-based case) divided by the total number of cells. It is interesting to note that the average downlink cell load resulting from the radio network planning, related to the SLBA-based RND, is 53.1% (Table VII) which is very close to 54.75%, as calculated in the SLBA-based RND (Table V). This is a good indication that capacity estimation in the SLBA-based RND is accurate for the considered scenario.

The SLBA-based dimensioning resulted in a network performance closer to the targets set; whereas the traditional approach resulted in 36% unnecessary additional eNBs, and incurred additional CapEX and OpEX. This is a clear indication to the importance of a suitable LTE RND, that is capable of capturing the intrinsic effects of the technology in an analytical and fast method. Accurate dimensioning results are vital to correct network deployment business modelling; it reduces business risks and advances the industry party ahead of competition. In addition, LTE RND helps cellular operators in deciding on reusable radio sites, additional radio sites, parameter setting, and network features. More importantly, it allows operators to make these decisions without disturbing network operation, hence sustaining quality of service and users satisfaction.

VII. Lessons Learned and Future Challenges

In this tutorial, we have followed the progress of radio network dimensioning from the target definition phase to the tool-based radio network planning phase. In every step, relevant concepts and derivations are presented with practical examples to provide a full understanding of the purpose, background, input, output and variations of the step. A statistical link budget analysis approach is described and applied to an LTE network model for sensitivity analysis. The study reveals LTE-specific characteristics that help understand the implication of different parameter settings and capture them in the dimensioning process. One such behaviour is the trade-off between cell loading and cell range distribution, framed as cell breathing and elasticity. Similarly, the impact of inter-site distance on cell edge coverage probability is captured, showing the delicate nature of LTE whereby a 100 meters difference degrades the edge user's quality drastically. The effect of power setting is also studied, with focus on a small cell scenario, showing an inflection point in the power curve that would provide the required SINR, and beyond which increasing the power becomes redundant. Consequently, the results from the sensitivity analysis lead the way towards presenting an iterative RND approach, based on statistical link budget analysis, to enable balancing conflicting constraints of coverage, capacity, and quality. A case study, comparing the statistical RND approach to the traditional RND, is presented, highlighting the risks of pragmatic assumptions (36% increase in CapEX and OpEX) and incentivising more research in the development of advanced LTE RND approaches.

But the fifth generation (5G) of cellular systems is being defined today and is expected to launch in 2020; it is partly an evolution of advanced 4G features, e.g., carrier aggregation, but also includes key novel disruptive technologies, as described in [49]. 5G design would have direct impact on RND procedures in which various features need to be accurately captured; in this section we address key 5G features and corresponding potential RND solutions. Heterogeneous networks (HetNets), presented in Section VII-A, are a prime 5G enabler. HetNets are basically an evolution of existing multi-layered networks with the inclusion of revolutionary technologies such as millimeter-wave (mmWave) radio access and massive MIMO, for instance. Cloud-RAN is another disruptive 5G technology, that is often considered with control/user plane split architecture, discussed in Section VII-B. The interaction between the backhaul/fronthaul and the RAN is becoming very tight to a point where a joint RAN and backhaul design and operation are required; this is explained in Section VII-C. Section VII-D, explores the impact of device-to-device (D2D) communication, including the role of smart devices such as mesh networking and caching. Machine to machine (M2M) communication is an essential part of 5G, and the network is expected to provision diverse services to a large spectrum of devices and applications, with different capabilities and requirements; all of that needs to be done in an efficient manner to cater for the one thousand fold of connected devices; the M2M RND problematic is presented in Section VII-E.

A. Heterogeneous networks with multiple radio access technologies

The concept of heterogeneous networks has been used in early generations of cellular networks under different names such as macro or umbrella layer/micro layer, or overlay/underlay cells, but has recently attracted a lot of attention in the advent of 5G [50], [51], [52]. In their new form, heterogeneous networks are composed of macro-cells, small cells, femto-cells, and WiFi

access points for traffic offloading, among other types of access points. Small cells are characterised by low transmit power, restricted coverage range, and dense deployment. Femto-cells are mostly indoor in residential and sometimes business environments, nevertheless their location is outside the control of the operator. The aim of heterogeneous networks is to push the traffic towards the smaller cells since they provide higher spectral efficiency due to their restricted coverage. Therefore, advanced features, such as cell range extension (CRE) and ABS, are included in release 10 to make small cells attractive to users [53] [54]. CRE essentially biases users to camping on small cells although the signal from the macro-cell might be higher; macro-cells use ABS on frames allocated to small cell edge users to reduce their interference. Such features will certainly affect capacity dimensioning, since some resources are unavailable to macro-cells, but are reused multiple times within their coverage areas through transmission over covered small cells. The implementation of these features is tightly related to the scheduling schemes and other radio access algorithms, which may be implementation dependent. One major challenge in heterogeneous networks, is capturing the inter-layer interference in different deployment scenarios. Authors in [55] propose an interference modelling in a multi-tier cell deployment, for the uplink interference, which can be used as an initial step towards HetNet capacity and coverage dimensioning. In [56], the authors present a survey of the usage of stochastic geometry in the modelling, analysis, and design of HetNets and cognitive networks. Indeed, stochastic geometry is a promising mathematical technique able to provide a rigorous analytical approach for estimating inter-layer interference, SINR, and cell outages. Discussing the issue of load balancing in HetNet deployment, the authors in [57] compare the usage of stochastic geometry to other methods (e.g., game theory) to maximise the system throughput by optimising the load balancing between small cells and macro-cells. These works certainly promote to utilisation of stochastic geometry in order to address major challenges such as modelling inter-layer ICI while accounting for small and large scale fading without approximations and without neglecting thermal noise. Such an analytical modelling of inter-layer ICI can then be used to derive expressions for RND related metrics such as interference margin and cell range.

Moreover, new access technologies are considered for small cells, and new spectrum bands are being explored based on millimeter waves (mmWave). Naturally, waves with smaller wavelength face more propagation challenges when used as cellular radio access; the spectrum in this range is however abundant and at low cost, if any. Nevertheless, knowing that the radio coverage of small cells is often limited to very small distances, in addition to the emergence of new technologies, such as 3D beamforming and massive MIMO from multi-element antenna arrays, small cells offer a plausible application for mmWave as radio access technology. Authors in [58] present a propagation modelling of mmWave radio access, an initial step in radio network dimensioning. Understanding propagation characteristic in these frequencies enables estimations of inter-cell interference and coverage ranges. Accordingly, the LBA should be modified according to these propagation characteristics for coverage dimensioning, and the capacity dimensioning should reflect the tighter reuse of the spectrum. Authors in [59], [60] propose a coverage and capacity analysis of mmWave cellular systems and mmWave Ad Hoc systems, respectively. In [59], they show that mmWave coverage may be comparable to microwave coverage, resulting in higher rate performance in view of the wider mmWave available bandwidth. Stochastic geometry is employed in [60] to characterize the coverage probability of a mmWave Ad Hoc network, which is found to exceed the area spectral efficiency

of lower frequency traditional Ad Hoc networks.

Small cells may have a cell range as small as ten meters, and hundreds of small cells are expected per square kilometer, in very dense areas [51]. Accordingly, roaming users would cross cell borders very often, thus, generating a crippling signalling load from cell reselection procedures and handovers. The concept of soft or phantom cell was introduced in LTE release 12, consisting of splitting the user and control planes. In this architecture, mobility is managed by the anchor cell (often the macro-cell) and the small cell is primarily used for data offloading. Consequently, handover and cell reselection are only triggered when users cross anchor cell borders, reducing the signalling loads significantly. Soft cells bring a new edge to the RND, because data signals and control channel signals are uncorrelated and need to be dimensioned separately to yield a balanced design. Firstly, traffic modelling needs to be re-assessed under the data/signalling planes split, because the traffic generated by one user will be distributed over the two layers, and perhaps additional control information would be required to manage the split. Consequently, capacity dimensioning should reflect the new traffic model on both data and signalling layers, knowing that a signalling cell covers more users than a data cell, but less traffic per user. From a coverage point of view, a user is considered covered if both the data and signalling channels are available, since an outage on any channel would result in an interrupted communication. Moreover, the radio access technology on each layer may be different, as well as the SINR target on each channel. On the other hand, both layers may be sharing the same spectrum, in this case inter-layer interference should be modelled based on the related traffic model. Otherwise, parallel LBAs should be conducted for each layer, where each captures the radio access technology specifics, propagation characteristics and supported service characteristics. Authors in [61] model the cell outage probability in heterogeneous networks with soft cells, and propose a cell outage management framework. Such an analysis may be the starting point of comprehensive heterogeneous network RND, with soft cells, whereby the network dimensions are re-adjusted until the outage targets on both layers are met.

Another related work looks at evaluating different deployment strategies (macro densification and small cells densification) in different types of cities [62]. Their method is based on well-known propagation models and evaluation methods, combining them to allow higher flexibility and improved accuracy, thus suitable for heterogeneous networks. Effectively, dimensioning heterogeneous networks, is not simply finding the radio site count of both macro and small cells separately; it also concerns finding the optimum split between both layers in such a way that network performance targets are met in a balanced way and at a minimum cost.

1) HetNet extended RND: Considering a HetNet system which consists of M macro-cells, and F femto-cells (or small cells), it is possible to extend the downlink RND approach described in this paper to incorporate the different network layers. Femto-cells are specially challenging because they are often deployed by the subscribers, thus their location is not decided by the cellular operator. Furthermore, femto-cells may be open access, i.e., may serve any subscriber, or may be closed-access in which case they are privately owned and corresponding capacity is exclusive to the owner. Moreover, the spectrum distribution among the different layers may be done in many ways, where the two extremes are: orthogonal versus unified spectrum allocation. In the former, the spectrum is segregated with an exclusive part of the spectrum allocated to the macro-cell and another to the femto-cell layer; the

bandwidth allocated to each may be, however, dynamically optimised. Whereas, in the unified spectrum, the spectrum is shared among all cells from all types; intelligent ICIC techniques need to be then used to control interference. The main advantage of the orthogonal spectrum allocation is that interference levels are kept at a minimum level, on the other hand, the unified spectrum allocation offers better utilisation of the spectrum.

The first milestone in RND is the evaluation and modelling of the interference levels in the network, as we did in (10). However, mutli-layer networks suffer from two types of interference: inter-layer interference (I_{inter}) and intra-layer interference (I_{intra}). The first is incurred from macro to femto-cell users or femto to macro-cell users; the other is macro to macro or femto to femto [63]. Thus, the interference modelling becomes more complex; we consider the two extreme spectrum allocation schemes, assuming open access femto-cells in both cases. The downlink interference is measured at the user's location, over the required sub-channel, and is the cumulative received signal strength, excluding the desired signal. There are two types of users is this case, those served by the macro-cells (MU's) and those served by the femto-cells (FU's); the corresponding measured interference levels by each type are shown below, where I_{MU} is the interference seen by a macro-cell user and I_{FU} is that seen by a femto-cell user.

$$I_{\text{MU}} = I_{\text{inter}} + I_{\text{intra}} = \sum_{m=1, m\neq s}^{M} S_{m,\text{MU}} + \sum_{f=1}^{F} S_{f,\text{MU}} \tag{33}$$

$$I_{\text{FU}} = I_{\text{inter}} + I_{\text{intra}} = \sum_{f=1, f\neq s}^{F} S_{f,\text{FU}} + \sum_{m=1}^{M} S_{m,\text{FU}} \tag{34}$$

where, $S_{x,u}$ is the received signal strength of the signal transmitted from cell x and received by user u, based on (2), and s indicates the serving cell index. The unified spectrum allocation incurs inter-layer interference that depends on the scheduling and ICIC mechanism in place; the general downlink interference can be expressed as above (33)-(34). In an orthogonal spectrum allocation scenario, cells in different layers do not re-use the same sub-channel, hence the corresponding received signal strength is nil, hence, the I_{intra} is also nil, as shown in (35)-(36) below.

$$I_{\text{MU}} = I_{\text{inter}} = \sum_{m=1, m\neq s}^{M} S_{m,\text{MU}} \tag{35}$$

$$I_{\text{FU}} = I_{\text{inter}} = \sum_{f=1, f\neq s}^{F} S_{f,\text{FU}} \tag{36}$$

Without loss of generality, downlink interference can thus be expressed as a summation of different downlink received signal strengths. Each of these signals has a fading component that is a random variable which follows known statistical distributions such as, Rayleigh or gamma distributions, hence the PDF of each received signal can be expressed as in (11) or (24), respectively. Mathematical techniques, such as the MGF approach, can then be used to find the PDF of the summation of random variables, as was done in the case of Rayleigh fading in (18), and for composite fading (modelled as a gamma distribution) in (26). As an alternative, stochastic geometry based methods can also be used to derive statistical models for the various interference terms. Once the distributions $f_{I_{\text{MU}}}(i)$ and $f_{I_{\text{FU}}}(i)$ are identified, then the statistical distribution of the corresponding interference

degradations $f_M^{\mathrm{MU}}(\mu)$ and $f_M^{\mathrm{FU}}(\mu)$ of each of the macro-cell and the femto-cell layers, respectively, can be derived using the relation in (21). Similarly, the statistical distributions of the MAPL and the cell range can be derived using the relations in (30) and (32), respectively. Given closed forms of the cell ranges distributions are found, it is then possible to conduct a detailed RND performance analysis for HetNets, and trigger an iterative process for dimensioning of the multi-layered network (e.g., by extending the iterative approach described in Figure 13), and trigger the iterative process to perform the dimensioning process of the multi-layered network.

B. Cloud-RAN

Cloud or *central* RAN, C-RAN, is another prime enabler to 5G networks. The concept is based on splitting the eNB functions and redistributing them between the RAN and the access point itself. The fully centralised RAN consists of migrating most functions toward the RAN and only leaving the radio frequency (RF) and analog-to-digital capabilities at the access point, otherwise referred to as remote RF head (RRH) as shown in Figure 17. The advantages of such an architecture are manyfold, related to reduction is cost and complexity of deployment and operation in addition to increase in efficiency of resource utilisation. These stem from the fact that lower complexity access points are lower cost and require less maintenance, and the centralised functions imply pooling of resources, such as the base band unit (BBU), hence, higher efficiency in usage (see Figure 17). The ”C” in C-RAN also refers to *cooperative* since it enables ease of implementation of advanced features that require inter-cell cooperation (e.g., ICIC and CoMP). Moreover, the centralised processing and inter-cell cooperation are exploited for green operation objectives, and reduced carbon footprints, thus the association of clean with the ”C”. Authors in [64] propose a user-centric virtual cell dimensioning, in which the radius of the virtual cell (a dynamic group of RRHs) is analysed for best system throughput. Indeed, capacity dimensioning with the C-RAN and pooled BBU differs greatly from the distributed RAN, in which the RND often addresses peak traffic per cell. The RRHs, are a form of small cells, thus, have limited footprint; traffic variation in small areas fluctuates drastically between peak highs and very low traffic. However, the dimensioning target has shifted from being cell-centric to BBU pool-centric, consequently increasing usage efficiency.

Nonetheless, the C-RAN architecture brings stringent capacity and latency requirements (up to 2.5Gbps [65] and as low as 150μsec [66], respectively) on the backhaul link between the RRH and the C-RAN, termed ”fronthaul”. Few current technologies can match these requirements, such as direct fibre; however, the incurred cost and inconvenience of laying fibre to every RRH renders the solution often infeasible. A fundamental change, inferred by the C-RAN architecture, is that there are no more clear boundaries between backhaul and radio, since the fronthaul is a vital connection between the separated functions of the traditional eNB. Accordingly, the backhaul dimensioning becomes a fundamental part of the 5G RND, as explained in Section VII-C.

Similarly, the evolution towards 5G is blurring the boundaries between network nodes and terminals. 5G devices can act as terminals, but also substitute for network nodes, such as relaying between other terminals and the C-RAN (i.e., provisioning the fronthaul). Section VII-D describes the device-to-device paradigm and how it affects the radio network dimensioning.

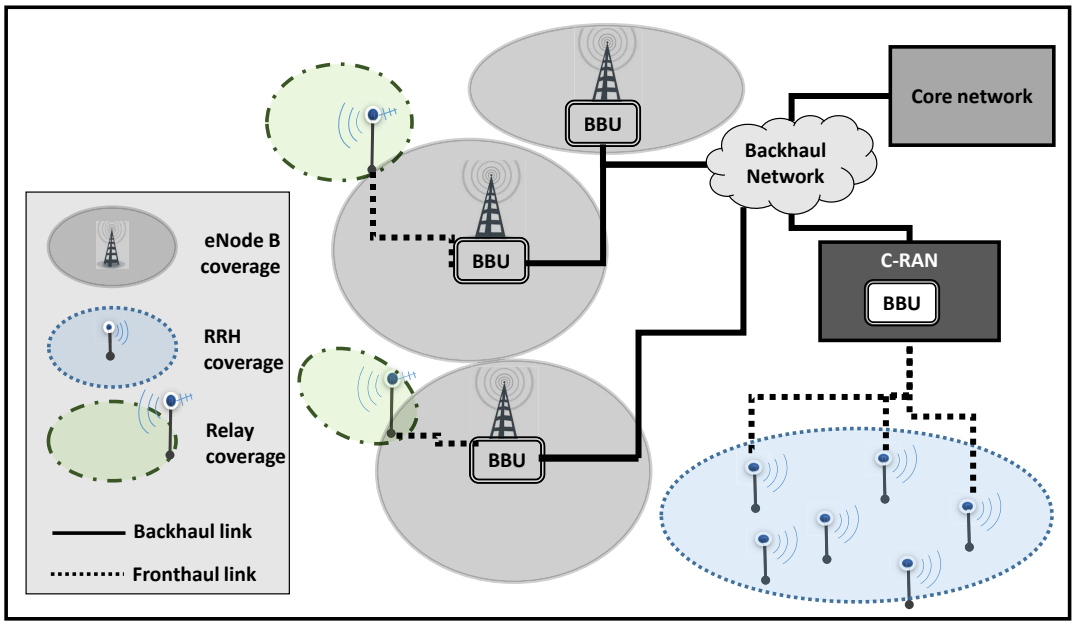

Fig. 17. The C-RAN architecture is a 5G enabler and uses RRH for BBU pooling and relays for coverage extension. The link connecting RRHs and relays to the BBU pool or donor cell, respectively, is called the fronthaul. Also, the C-RAN can co-exist with traditional cells.

C. Backhaul/fronthaul considerations

The backhaul, conventionally, refers to the connection between the radio site and the core network, and is usually provided using fibre or microwave links. In the advent of the C-RAN, and related stringent capacity and latency requirements, these solutions are either not suitable, not available or too costly, which brings innovative replacements. The term backhaul, with C-RAN architecture, refers to transport network comprising both the fronthaul and the traditional backhaul. Authors in [51] proposed a backhaul toolbox, including legacy and innovative solutions, to suit different cellular deployments. One solution under investigation is using millimeter-wave for connecting small cells to a transport hub, potentially the radio site [51]. Millimeter-wave offers wide spectrum at the cost of fragile connectivity, where line of sight is required but may be disturbed by pole swaying or rainfall. A measurement campaign on mmWave propagation, as radio access and backhaul access, was conducted in New York City, showing 16% outage probability for mmWave backhaul links [58]. Another discussed solution is in-band backhaul; i.e., the LTE radio bandwidth in a macro-cell will be shared between LTE users and backhaul connections to small cells. This solution is attractive since it does not require installing new equipment, and propagation in this band is reliable, without the need of line of sight; however it brings additional constraints to the already crowded spectrum. Nonetheless, for most wireless (mmWave, in-band, or WiFi, etc.) or wired (e.g., fibre to the node with copper to the premise) fronthaul solutions, the relative capacity and latency depend on the length of the link. Accordingly, it is essential to develop a fronthaul-aware RND, since the fronthaul may result in a network performance bottleneck otherwise. Self organised capabilities are used, in [67], for capacity dimensioning of heterogeneous networks with in-band fronthaul. Small cells use self-optimising techniques to adapt the resource allocation based on changing traffic scenarios, in order to maximise the system capacity. In this case, backhauling affects both capacity and coverage dimensioning of heterogeneous networks by contributing to the interference level and competing for the shared capacity. From a different perspective, authors in [68] analyse how the backhaul delay affects the performance of heterogeneous networks, for different deployments using wired, in-band, and wireless

backhauling. The paper demonstrates that network densification without backhaul considerations could deteriorate the performance of the network due to high delays.

In fact, interworking and joint design of radio access and backhaul is considered a prime enabler to 5G networks, as promoted by the JOIN group in [69]. The authors analyse the challenges of jointly designing the radio access and backhaul in a C-RAN architecture. The challenges in the network layer concern user-cell association, which is no longer based on signal strength, but takes also into consideration issues such as backhaul constraints, energy efficiency, and load balancing. Authors from the same group study the problem of joint resource allocation between backhaul and radio access links in time division multiplexing, and propose a scheme that improves network performance significantly, specially with the usage of dynamic clustering for inter-cell interference coordination [70]. Owing to the increasing need for joint radio and backhaul design, an appropriate future 5G heterogeneous network RND exercise requires information related to backhaul capacity, latency, reliability and energy consumption for deciding on the macro-cell and small cell count and relative parameters. Small cells will only absorb traffic if the fronthaul/backhaul is capable of supporting it, thus their cell range is limited by the backhaul conditions, in addition to legacy considerations, e.g., radio access coverage, capacity and quality .

D. Device-to-device (D2D) connectivity

Traditionally, users in a cellular network communicate with each other through pre-deployed network nodes; in 5G it is envisaged that devices, served by the network, are able to communicate among each other directly, thus acting as relays and potentially creating a massive ad hoc mesh network [71]. Authors in [72] propose an algorithm that finds a D2D density and power allocation, based on network conditions, to maximise the D2D achievable transmission capacity. This is typically a D2D dimensioning exercise, in which the number of devices and associated power are found, in an out-band D2D commination scenario. In [73], D2D communication is exploited from a proactive caching approach, whereby, influential users are identified, and used for caching popular files. Consequently, D2D communication is used to transmit the data to other users, with good quality of experience, while avoiding network congestion and alleviating backhaul requirements. This type of D2D usage, requires revisiting the traffic modelling to incorporate the off-peak caching traffic on one hand, and the reduction of peak radio access traffic on the other hand, affecting both coverage and capacity dimensioning. Accordingly, planning with D2D transforms RND of cellular networks to that of ad hoc mesh networks, thus bringing many new challenges to the planning exercise. A major challenge is to model the D2D traffic, based on D2D usage (e.g., for caching, coverage extension, etc.) over different radio access technologies (in-band for device to/from eNB and in-band/out-band for D2D). This information is key to capacity and coverage dimensioning. Devices used as a relay can increase the cell range predicted by the LBA; however, the location and capabilities of these devices need to be known for the coverage dimensioning. In such a case, the link budget can be designed for a lower SINR, assuming that devices with better SINR will relay to users at the cell edge. If D2D communication is in-band (i.e., reuses the same spectrum as the radio access), interference from

these links needs to be estimated and would affect both coverage and capacity dimensioning.

Devices may also be planned by operators at fixed locations thus forming fixed relays, a form of small cell deployment enabling 5G, used to increase the network capacity or extend the coverage as shown in Figure 17 [74]. The relay, thus, becomes a small cell, and its link to the donor cell is the fronthaul, which is either in-band, if the relay shares the bandwidth with donor cell users, or out-band otherwise. Authors in [75] study the benefits of relays in three different scenarios: wired, in-band, and mmWave fronthaul. Their results show that in-band fronthaul may result in negative gains, and promote the usage of mmWave for the wireless fronthaul instead. Authors in [76] investigate planning relays to support traffic in 5G networks with carrier aggregation. They perform a dimensioning exercise to determine the number of needed relays, and the number of wireless channels that should be used by each relay to schedule data transmissions. Similar to unplanned D2D RND challenges, fixed relays require re-modelling of traffic and D2D interference estimation based on D2D/fronthaul spectrum. Given this information, the coverage dimensioning would incorporate relay-enabled extensions, and the capacity dimensioning would take into consideration sharing the spectrum with the fronthaul and the D2D traffic model.

Full duplex (FD) is a promising technique for implementing in-band D2D communication. It enables a device to transmit and receive simultaneously, thus, can potentially double the spectral efficiency in the physical layer. Authors in [77] analyse the advantages of FD is heterogeneous networks by integrating FD radios in small cells and allowing D2D underlay communications in parallel. However merits of FD can only be reaped with advanced self-interference cancellation techniques, as detailed in [78] among other challenges such as: size of the device, channel estimation, and joint resource management across layers. FD has ignited intensive research, such as [79], in which authors look at maximising the end-to-end performance by joint optimisation of the power control and beamforming at the relay. Radio network dimensioning with FD is certainly challenging and requires focused attention; authors in [80] propose an analytical analysis of the outage performance of coherent partial decode-forward relaying over small scale fading channels in both half and full duplex transmissions. Outage performance is the first step in RND; the objective would be to adjust the network design (macro-cell and D2D count and corresponding parameters) to meet the outage targets for both coverage and capacity.

E. Machine to machine (M2M) communication

Machine-to-machine (M2M) communication refers to machine type devices (MTC) that communicate among each other, or with an application platform, through the cellular network. M2M applications are diverse and different; some are fixed locations, such as sensors and security devices, others are mobile such as health devices and fleet-tracking devices. Nonetheless, it is anticipated that massive M2M deployment will create a landslide to cellular networks; a major factor necessitating network densification. However, M2M communication requirements differ greatly from conventional human-to-human (H2H) communication. They are mostly characterised by low data volume but bring stringent constraints such as underground device location in the case of smart

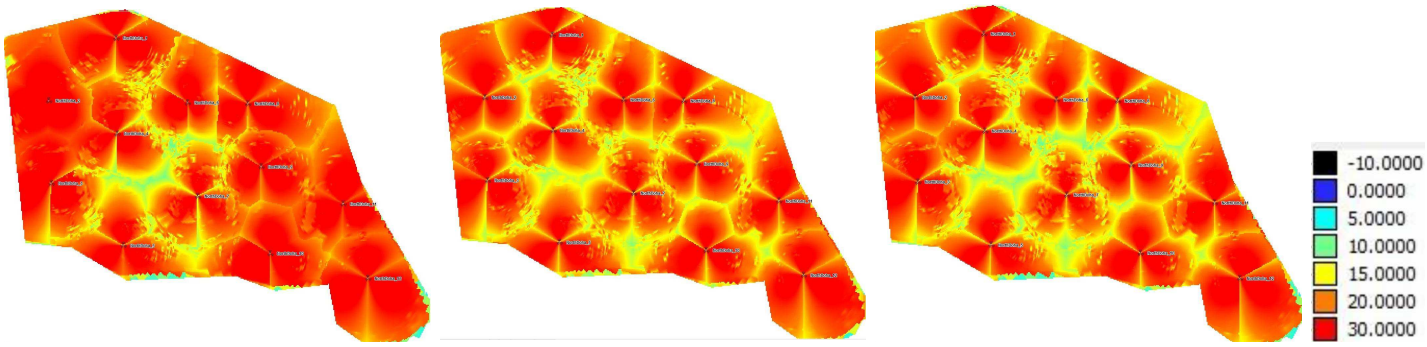

(a) H2H only. (b) H2H with smart meters. (c) H2H with smart meters and fleet M2M. (d) Legend.

Fig. 18. SINR (dB) plot of downlink reference signal for the three considered scenarios, showing degradation when M2M services are introduced.

meters, or no tolerance to delay in case of security or medical systems, for example. It is possible that an RND design using the approach proposed in this tutorial proves suitable for H2H users, but would fail to cover smart meters located in difficult areas, for instance. With M2M requirements set as design targets in the coverage and capacity analysis, the planning results will surely differ from the traditional H2H planning approach. The challenge resides in reconciling between planning designs dictated by human operated smart phones and those imposed by M2M devices.

Other challenges in network planning stem from the M2M device characteristics. A recent study item [81] on low-cost and enhanced coverage for MTC devices has been initiated with the purpose of facilitating the LTE/LTE-A usage of M2M communications from an economical perspective. Thus, in order to reduce the cost of machines, lower requirements are defined for the transmit/receive capabilities of the devices. The study gives an insight to M2M device characteristics; pertinent parameters to radio planning include: single receive antenna; reduced transmit power; limited energy storage capabilities; reduced peak data rate of 1Mbps; device noise figure 9dB; reduced bandwidth with baseband data channel of 1.4MHz; coverage enhancement of at least 15dB (using techniques such as antenna beamforming) basically to compensate for loss in coverage of low cost devices in restricted coverage areas (such as underground smart meters).

It is certainly a challenge to capture this new dimension in the RND procedure, which may necessitate solving for several statistical link budget analysis jointly to find a balanced design that mitigates H2H and D2D design requirements. A preliminary study was undertaken, using commercial LTE cellular planning tool, to highlight the effect of M2M traffic on the network; it considers three scenarios: H2H, H2H with smart meters, H2H with smart meters and fleet tracking M2M. Figure 18 shows the degradation of downlink reference signal SINR upon the introduction of M2M services in the network. Figure 19 shows the uplink data SINR severe deterioration when M2M services are enabled. H2H traffic is typically downlink heavy, however, M2M's uplink traffic is often dominant. For this reason, the uplink SINR is drastically affected by M2M services, whereas, the downlink degradation is more moderate. These results clearly highlight the need to account for M2M considerations in both dimensioning and network planning phases. Thus, it is essential to equip network operators with an M2M aware RND approach, since accounting for M2M in early planning stages would certainly reduce costly post-deployment rectifications.

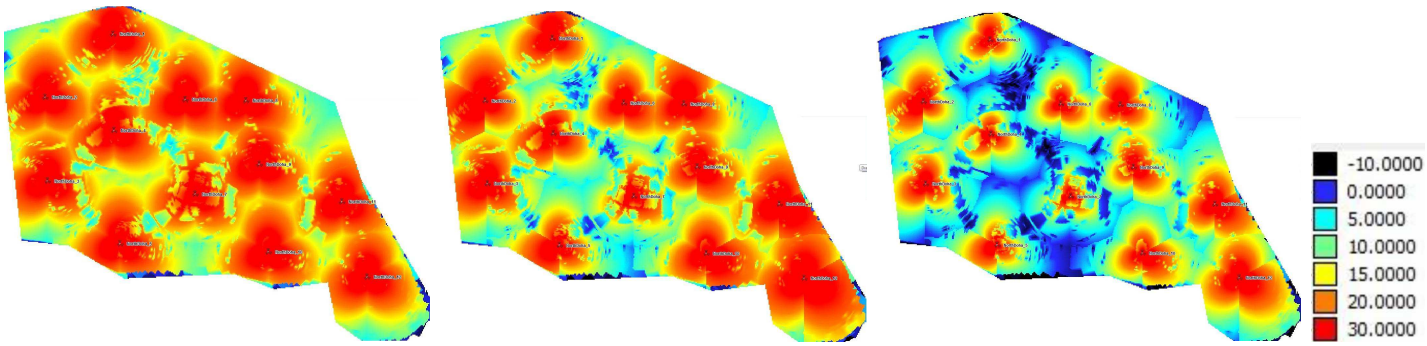

(a) H2H only. (b) H2H with smart meters. (c) H2H with smart meters and fleet M2M. (d) Legend.

Fig. 19. SINR (dB) plot of uplink data channel for the three considered scenarios, showing severe degradation when M2M services are introduced.

ACKNOWLEDGMENT

This work was made possible by NPRP grant $\#4 - 353 - 2 - 130$ from the Qatar National Research Fund (a member of The Qatar Foundation). The statements made herein are solely the responsibility of the authors.

REFERENCES

[1] L. Al-Kanj, Z. Dawy, and G. Turkiyyah, "A mathematical optimization approach for radio network planning of GSM/UMTS co-siting," in *IEEE International Conference on Communications (ICC)*, (Dresden, Germany), Jun 2009.

[2] Ofcom, "UK 3G mobile services data 2013." [Online], Available: http://maps.ofcom.org.uk/mobile-services/mobile-services-data-3G/, 2013.

[3] D. González G and J. Hämäläinen, "Looking at cellular networks through canonical domains and conformal mapping," *arXiv preprint arXiv:1505.01988*, 2015.

[4] J. Lempiinen and M. Manninen, *Radio Interface System Planning for GSM/GPRS/UMTS*. Springer, 1st ed., 2001.

[5] H. Holma and A. Toskala, *WCDMA for UMTS: HSPA Evolution and LTE*. Wiley, 5th ed., 2010.

[6] H. Holma and A. Toskala, *LTE for UMTS: Evolution to LTE-Advanced*. Wiley, 2nd ed., 2011.

[7] A. Abdel Khalek, L. Al-Kanj, Z. Dawy, and G. Turkiyyah, "Optimization models and algorithms for joint uplink/downlink UMTS radio network planning with SIR-based power control," *IEEE Transactions on Vehicular Technology*, vol. 60, no. 4, pp. 1612–1625, May 2011.

[8] B. Upase, M. Hunukumbure, and S. Vadgama, "Radio network dimensioning and planning for WiMAX networks," *Fujitsu Scientific Technical Journal*, vol. 43, no. 4, pp. 435–450, 2007.

[9] L. Decreusefond, E. Ferraz, P. Martins, and T. Vu, "Robust methods for LTE and WiMAX dimensioning," in *6th International Conference on Performance Evaluation Methodologies and Tools (VALUETOOLS)*, Oct 2012.

[10] Ibrahim, K.M. et al., "LTE dimensioning tool using C#," in *9th International Conference on Computer Engineering Systems (ICCES)*, (Cairo, Egypt), Dec 2014.

[11] Charles, J., "Refined statistical analysis of evolution approaches for wireless networks," *IEEE Transactions on Wireless Communications*, vol. 14, May 2015.

[12] F. Furqan, D. Hoang, and I. Collings, "Effects of quality of service schemes on the capacity and dimensioning of LTE networks," in *IEEE International Performance Computing and Communications Conference (IPCCC)*, (Austin, Texas, U.S.A.), Dec 2014.

[13] A. Fernekess, A. Klein, B. Wegmann, K. Dietrich, and M. Litzka, "Load dependent interference margin for link budget calculations of OFDMA networks," *IEEE Communications Letters*, vol. 12, no. 5, pp. 398–400, May 2008.

[14] A. B. Syed, "Dimensioning of LTE network, description of models and tool, coverage and capacity estimation of 3GPP long term evolution, radio interface," Master's thesis, Dept. Electrical and Communications Engineering, Helsinki University of Technology, Espoo, Finland, Feb 2009.

[15] A. Salo, M. Nur-Alam, and K. Chang, "Practical introduction to LTE radio planning." [Online], Available: http://digitus.itk.ppke.hu, Nov 2010.

[16] C. Seol and K. Cheun, "A statistical intercell interference model for downlink cellular OFDMA networks under log-normal shadowing and multipath Rayleigh fading," *IEEE Transactions on Communications*, vol. 57, no. 10, pp. 3069–3077, Oct 2009.

[17] C. Seol and K. Cheun, “A statistical intercell interference model for downlink cellular OFDMA networks under log-normal shadowing and multipath Ricean fading,” *IEEE Communications Letters*, vol. 14, no. 11, pp. 1011–1013, Nov 2010.

[18] D. Ben Cheikh, J. M. Kelif, M. Coupechoux, and P. Goldewski, “SIR distribution analysis in cellular networks considering the joint impact of path-loss, shadowing and fast fading,” *EURASIP Journal on Wireless Communications and Networking*, DOI:10.1186/1687-1499-2011-137, Oct 2011.

[19] H. Tabassum *et al.*, “An intercell interference model based on scheduling for future generation wireless networks (part 1 and part 2),” *arXiv preprint arXiv:1206.2292*, 2012.

[20] X. Yang and A. Fapojuwo, “Coverage probability and spectral efficiency for downlink hexagonal cellular networks with Rayleigh fading,” in *IEEE 24th International Symposium on Personal Indoor and Mobile Radio Communications (PIMRC)*, (London, U.K.), Sept 2013.

[21] J. G. Andrews, F. Baccelli, and R. K. Ganti, “A tractable approach to coverage and rate in cellular networks,” *IEEE Transactions on Wireless Communications*, vol. 59, no. 11, pp. 3122–3134, Nov 2011.

[22] E. Yaacoub and Z. Dawy, “Joint uplink scheduling and interference mitigation in multicell LTE networks,” *IEEE International Conference on Communications (ICC)*, 2011.

[23] R. Giuliano and F. Mazzenga, “Dimensioning of OFDM/OFDMA-based cellular networks using exponential effective SINR,” *IEEE Transactions on Vehicular Technology*, vol. 58, no. 8, pp. 4204–4213, Oct 2009.

[24] Nortel Networks, “Effective SIR computation for OFDM system-level simulations,” in *3GPP TSG RAN WG1 Meeting*, vol. 35, (Lisbon, Portugal), Nov 2003.

[25] WiMAX forum, “WiMAX system evaluation methodology.” version 2.1, Jul 2008.

[26] J. Kelif, M. Coupechoux, and P. Godlewski, “On the dimensioning of cellular OFDMA networks,” *Physical Communication*, vol. 5, no. 1, pp. 10–21, Mar 2012.

[27] T. S. Rappaport *et al.*, *Wireless communications: principles and practice*, vol. 2. prentice hall PTR New Jersey, 1996.

[28] Gilhousen, K. S. et al., “On the capacity of a cellular CDMA system,” *IEEE Transactions on Vehicular Technology*, vol. 40, no. 2, pp. 303–312, 1991.

[29] D. Reudink, *Microwave Mobile Communications*, ch. 2, pp. 126–128. IEEE Press, edited by Jakes, W.C. ed., 1993.

[30] M. Hata, “Empirical formula for propagation loss in land mobile radio services,” *IEEE Transactions on Vehicular Technology*, vol. VT-29, no. 3, pp. 317–325, Aug 1980.

[31] Z. Dawy, S. Jaranakaran, and S. Sharafeddine, “Intercell interference margin for CDMA uplink radio network planning,” in *15th IEEE International Symposium on Personal, Indoor and Mobile Radio Communications, PIMRC*, vol. 4, pp. 2840–2844 Vol.4, Sept 2004.

[32] G. Llano, J. Reig, and L. Rubio, “Analytical approach to model the fade depth and the fade margin in UWB channels,” *IEEE Transactions on Vehicular Technology*, vol. 59, pp. 4214–4221, Nov 2010.

[33] P. Zhao, Y. Zhang, S. Zhou, and Y. Hu, “A new method of obtaining slow fading characteristics from CW test and its implementations in radio planning,” in *IEEE International Conference on Communications Technology and Applications, ICCTA ’09.*, pp. 279–283, Oct 2009.

[34] E. Pateromichelakis, M. Shariat, A. Quddus, and R. Tafazolli, “On the evolution of multi-cell scheduling in 3GPP LTE / LTE-A,” *IEEE Communications Surveys Tutorials*, vol. 15, pp. 701–717, Second quarter 2013.

[35] S.-H. Moon, C. Lee, S.-R. Lee, and I. Lee, “Joint user scheduling and adaptive intercell interference cancelation for MISO downlink cellular systems,” *IEEE Transactions on Vehicular Technology*, vol. 62, pp. 172–181, Jan 2013.

[36] F. Hu, K. Zheng, L. Lei, and W. Wang, “A distributed inter-cell interference coordination scheme between femtocells in LTE-dvanced networks,” in *IEEE 73rd Vehicular Technology Conference (VTC Spring)*, pp. 1–5, May 2011.

[37] E. Yaacoub, A. Imran, and Z. Dawy, “A generic simulation-based dimensioning approach for planning heterogeneous LTE cellular networks,” in *17th IEEE Mediterranean Electrotechnical Conference (MELECON)*, Apr 2014.

[38] Z. Qinjuan, G. Lin, S. Can, A. Xudong, and C. Xiaochen, “Joint power control and component carrier assignment scheme in heterogeneous network with carrier aggregation,” *Communications, IET*, vol. 8, pp. 1831–1836, Jul 2014.

[39] M. Jaber, N. Akl, Z. Dawy, and E. Yaacoub, “Statistical link budget analysis approach for LTE cellular network dimensioning,” *Proceedings of 20th European Wireless Conference*, 2014.

[40] W. El-Beaino, A. El-Hajj, and Z. Dawy, "A proactive approach for LTE radio network planning with green considerations," in *19th International Conference on Telecommunications (ICT)*, (Jounieh, Lebanon), Apr 2012.

[41] S. Al-Ahmadi and H. Yanikomeroglu, "On the approximation of the generalized-K distribution by a gamma distribution for modeling composite fading channels," *IEEE Transactions on Wireless Communications*, vol. 9, no. 2, pp. 706–713, Feb 2010.

[42] H. Tabassum, F. Yilmaz, Z. Dawy, and M.-S. Alouini, "A framework for uplink intercell interference modeling with channel-based scheduling," *IEEE Transactions on Wireless Communications*, vol. 12, pp. 206–217, Jan 2013.

[43] H. Tabassum, F. Yilmaz, Z. Dawy, and M. Alouini, "On the modeling of uplink inter-cell interference based on proportional fair scheduling," in *IEEE Wireless Communications and Networking Conference Workshops (WCNCW)*, (Paris, France), Apr 2012.

[44] H. Tabassum, F. Yilmaz, Z. Dawy, and M.-S. Alouini, "A statistical model of uplink inter-cell interference with slow and fast power control mechanisms," *IEEE Transactions on Communications*, vol. 61, pp. 3953–3966, Sept 2013.

[45] H. Tabassum, Z. Dawy, M. Alouini, and F. Yilmaz, "A generic interference model for uplink OFDMA networks with fractional frequency reuse," *IEEE Transactions on Vehicular Technology*, vol. 63, pp. 1491–1497, Mar 2014.

[46] Forsk, "Atoll." [Online], Available:http://www.forsk.com/atoll/.

[47] TEOCO, "Asset." [Online], Available:http://www.teoco.com/products/planning-optimization/asset-radio-planning.

[48] InfoVista, "Mentum Planet." [Online], Available:http://www.infovista.com/products/Radio-Access-Network-planning-and-optimization.

[49] F. Boccardi, R. Heath, A. Lozano, T. Marzetta, and P. Popovski, "Five disruptive technology directions for 5G," *IEEE Communications Magazine*, vol. 52, pp. 74–80, Feb. 2014.

[50] 3GPP TS 36.932, "Scenarios and requirements for small cell enhancements for E-UTRA and E-UTRAN (Release 12)," tech. rep., 2013.

[51] Small Cell Forum, "Backhaul Technologies for Small Cells: Use Cases, Requirements and Solutions." [Online], Available: http://www.scf.io/en/documents, Feb 2013.

[52] NGMN Alliance, "Small cell backhaul requirements." [Online], Available: http://www.ngmn.org/uploads/media/NGMN-Whitepaper-Small-Cell-Backhaul-Requirements.pdf, Jun 2012.

[53] Panasonic, "R1-113806: Performance study on ABS with reduced macro power," in *3GPP TSG RAN WG1 Meeting*, vol. 67, (San Fransisco, U.S.A.), Nov 2011.

[54] Qualcomm Europe, "R1-083813:Range expansion for efficient support of heterogeneous networks," in *3GPP TSG RAN WG1 Meeting*, vol. 54bis, (Prague, Czech Republic), Sept 2008.

[55] H. Tabassum, Z. Dawy, E. Hossain, and M.-S. Alouini, "Interference statistics and capacity analysis for uplink transmission in two-tier small cell networks: A geometric probability approach," *IEEE Transactions on Wireless Communications*, vol. 13, pp. 3837–3852, Jul 2014.

[56] H. Elsawy, E. Hossain, and M. Haenggi, "Stochastic geometry for modeling, analysis, and design of multi-tier and cognitive cellular wireless networks: A survey," *IEEE Communications Surveys and Tutorials*, vol. 15, pp. 996–1019, Third 2013.

[57] J. Andrews, S. Singh, Q. Ye, X. Lin, and H. Dhillon, "An overview of load balancing in hetnets: old myths and open problems," *Wireless Communications, IEEE*, vol. 21, pp. 18–25, Apr 2014.

[58] S. Rangan, T. Rappaport, and E. Erkip, "Millimeter-wave cellular wireless networks: Potentials and challenges," *Proceedings of the IEEE*, vol. 102, pp. 366–385, Mar 2014.

[59] S. Akoum, O. El Ayach, and R. Heath, "Coverage and capacity in mmWave cellular systems," in *Conference Record of the 46th Asilomar Conference on Signals, Systems and Computers (ASILOMAR)*, pp. 688–692, Nov. 2012.

[60] A. Thornburg, T. Bai, and R. Heath, "MmWave Ad Hoc network coverage and capacity," in *IEEE International Conference on Communications (ICC)*, pp. 1310–1315, Jun. 2015.

[61] Onireti, O. et al., "A cell outage management framework for dense heterogeneous networks," *IEEE Transactions on Vehicular Technology*, no. 99, pp. 1–1, 2015. Accepted for publication in a future issue of this journal.

[62] Charles, J. et al., "Refined statistical analysis of evolution approaches for wireless networks," *IEEE Transactions on Wireless Communications*, vol. 14, pp. 2700–2710, May 2015.

[63] *Interference analysis in a LTE-A HetNet scenario: Coordination vs. uncoordination*, Jun 2013.

[64] Y. Zhang and Y. J. Zhang, "User-centric virtual cell design for Cloud Radio Access Networks," in *IEEE 15th International Workshop on Signal Processing Advances in Wireless Communications (SPAWC)*, (Toronto, Canada), pp. 249–253, Jun 2014.

[65] Maeder, A. et al., "Towards a flexible functional split for cloud-RAN networks," in *European Conference on Networks and Communications (EuCNC)*, (Bologna, Italy), Jun 2014.

[66] Dotsch, U. et al., "Quantitative analysis of split base station processing and determination of advantageous architectures for LTE," *Bell Labs Technical journal*, vol. 18, pp. 105 – 128, Jun 2014.

[67] R. Combes, Z. Altman, and E. Altman, "Self-organizing relays: Dimensioning, self-optimization, and learning," *IEEE Transactions on Network and Service Management*, vol. 9, pp. 487–500, Dec 2012.

[68] D. Chen, T. Quek, and M. Kountouris, "Backhauling in heterogeneous cellular networks: Modeling and tradeoffs," *IEEE Transactions on Wireless Communications*, 2015. accepted for publication in a future issue of this journal.

[69] Bernardos, C.J. et al, "Challenges of designing jointly the backhaul and radio access network in a cloud-based mobile network," *Future Network and Mobile Summit (FutureNetworkSummit)*, Jul 2013.

[70] M. Shariat, E. Pateromichelakis, A. Quddus, and R. Tafazolli, "Joint TDD backhaul and access optimization in dense small cell networks," *IEEE Transactions on Vehicular Technology*. Accepted for publication in a future issue of this journal.

[71] M. Tehrani, M. Uysal, and H. Yanikomeroglu, "Device-to-device communication in 5G cellular networks: challenges, solutions, and future directions," *IEEE Communications Magazine*, vol. 52, pp. 86–92, May 2014.

[72] Z. Liu, T. Peng, H. Chen, and W. Wang, "Transmission capacity of D2D communication under heterogeneous networks with multi-bands," in *IEEE 77th Vehicular Technology Conference (VTC Spring)*, pp. 1–6, Jun 2013.

[73] E. Bastug, M. Bennis, and M. Debbah, "Living on the edge: The role of proactive caching in 5G wireless networks," *IEEE Communications Magazine*, vol. 52, pp. 82–89, Aug 2014.

[74] iJoin, "D2.1: State of the art of and promising candidates for PHY layer approaches on access and backhaul network." [Online], Available: http://www.ict-ijoin.eu/wp-content/uploads/2014/01/D2.1.pdf, Nov 2013.

[75] J. Ghimire, C. Rosenberg, and S. Periyalwar, "Why are relays not always good for you? Performance of different relay deployment configurations in a heterogeneous network," in *12th International Symposium on Modeling and Optimization in Mobile, Ad Hoc, and Wireless Networks (WiOpt)*, (Hammamet, Tunisia), pp. 333–340, May 2014.

[76] E. Yaacoub and Z. Dawy, "On using relays with carrier aggregation for planning 5G networks supporting M2M traffic," in *IEEE 10th International Conference on Wireless and Mobile Computing, Networking and Communications (WiMob)*, (Larnaca, Cyprus), Oct 2014.

[77] Wang, L. et al., "Exploiting full duplex for device-to-device communications in heterogeneous networks," *IEEE Communications Magazine*, vol. 53, pp. 146–152, May 2015.

[78] Liu, G. et al., "In-band full-duplex relaying: A survey, research issues and challenges," *IEEE Communications Surveys Tutorials*, vol. 17, pp. 500–524, Secondquarter 2015.

[79] G. Zheng, "Joint beamforming optimization and power control for full-duplex MIMO two-way relay channel," *IEEE Transactions on Signal Processing*, vol. 63, pp. 555–566, Feb 2015.

[80] A. Abu Al Haija and M. Vu, "Outage analysis for coherent decode-forward relaying over rayleigh fading channels," *IEEE Transactions on Communications*, vol. 63, pp. 1162–1177, Apr 2015.

[81] 3GPP TS 36.888, "Study on provision of low-cost Machine-Type Communications (MTC) User Equipments (UEs) based on LTE," tech. rep., 2013.